Electronic Supplementary Material (ESI) for Chemical Communications.
This journal is © The Royal Society of Chemistry 2023

Competition Between Side-Chain Interactions Dictates 2D Polymer Stacking Order

Alexander K. Oanta, Chloe E. Pelkowski, Michael J. Strauss, and William R. Dichtel*

Department of Chemistry, Northwestern University, Evanston, Illinois 60208, United States

Supporting Information

Correspondence Address
Professor William R. Dichtel Department of Chemistry Northwestern University 2145 Sheridan Road Evanston, IL 60208 (USA) wdichtel@northwestern.edu

Table of Contents

List of Figures in Supporting Information

A. Materials and Methods

Materials

All chemicals were either purchased from Sigma Aldrich or Tokyo Chemical Industries and used as received or synthesized using procedures adapted from literature reports as noted.

Methods and Instrumentation

Nuclear Magnetic Resonance. All ^{1}H NMR spectra were collected at 298 K on a Bruker Avance III 500 MHz spectrometer. Chemicals shifts were calibrated using residual NMR solvent ($CDCl_3$ at 7.26 ppm and DMSO-d_6 at 2.50 ppm) as an internal reference. Solid state cross-polarization magic angle spinning (CP-MAS) ^{13}C NMR spectra were collected on a 400 MHz Bruker Avance III HD NMR spectrometer with a 4 mm HX probe. The spinning rate at the magic angle was 10 kHz at 298 K. The Bruker pulse sequence of cross-polarization was used with standard proton decoupling. The spectrum was referenced to adamantane at δ 38.3 ppm.

High-Resolution Mass Spectrometry. HR-MS data was gathered by an Agilent 6210A LC-TOF mass spectrometer, with Atmospheric Pressure Photoionization (APPI) as an ionization source. The mass spectrometer was fitted with an Agilent 1200 HPLC binary pump and an autosampler. The samples were run on this instrument using the direct injection method.

Sonication. Sonication was performed with a Branson 3510 sonicator that was set to a frequency of 42 kHz and a power output of 100 W.

Supercritical CO_2 Drying. Supercritical drying was performed with a Leica EM CPD300 critical point dryer using bone-dry grade CO_2. After samples were loaded into the drying chamber in teabags (ETS Drawstring Tea Filters, sold by English Tea Store) that had been pre-soaked in methanol or acetone, the drying chamber was cooled to 15 °C and filled with CO_2. Subsequently, the CO_2 within the chamber was exchanged 80 times, and finally, the temperature was raised to 40 °C before the system was vented to release pressure.

Nitrogen Porosimetry. Nitrogen gas adsorption isotherms were collected with a Micromeritics ASAP 2420 accelerated surface area and porosity analyzer. 20-30 mg of 2DP samples were loaded into pre-massed dry analysis tubes fitted with filler rods and Transeal caps. The samples were heated to 40 °C at a rate of 1 °C/min and evacuated at 40 °C for 20 minutes, then heated to 100 °C at a rate of 1 °C/min and evacuated at 100 °C for 18 h. After degassing, each sample was weighed again to determine the mass of the activated sample, found by subtracting the initial mass. Then, adsorption measurements were run using UHP-grade N_2, generated by incremental exposure of N_2 up to 1 atm in a liquid nitrogen bath. Surface areas were determined by the BET model (calculated from the linear region of the N_2 isotherm within the pressure ranges shown in the BET plots below) and pore width distributions were determined using DFT models, all found using the instrument software.

Fourier-Transform Infrared Spectroscopy. FT-IR spectra were acquired at room temperature on a Nicolet iS10 FT-IR instrument using a ZnSe ATR attachment and 4 cm^{-1} resolution.

Powder X-ray Diffraction and Simulations. Powder X-ray diffraction patterns were collected at room temperature using a STOE STADI P powder diffractometer with CuKα1 radiation (λ = 1.54056 Å). The 2DP samples were placed between acetate foils, mounted into a rotating holder, and measured in transmission geometry mode. Materials Studio (version 5.0) was used to generate simulated PXRD patterns. For each series of 2DPs, an initial 2DP structure was drawn, and the Forcite Module was employed to optimize first the geometry, then the energy, of the structure using parameters from the Universal Force Field. Afterward, the Reflex module was used to generate PXRD patterns. These predicted PXRD patterns were then compared to experimental data. The unit cell parameters were also obtained from these optimized structures.

B. Synthetic Procedures

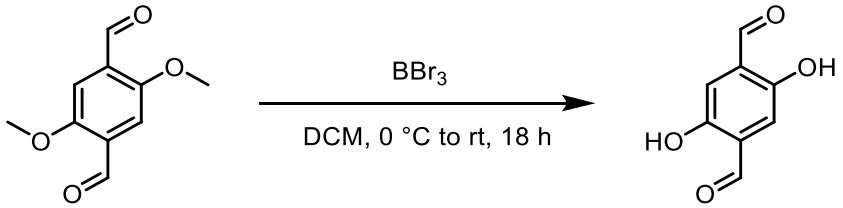

Synthesis of 2,5-dihydroxy-1,4-dibenzaldehyde.[1] 2,5-dimethoxy-1,4-dibenzaldehyde (3.0 g, 15 mmol, 1.0 equiv) was added to dry CH_2Cl_2 (150 mL) in a flame-dried 250 mL round bottom flask. The atmosphere was flushed with N_2, and the reaction flask cooled to 0 °C before BBr_3 (1.0 M in CH_2Cl_2, 42 mL, 42 mmol, 2.8 equiv) was added dropwise. The reaction was allowed to warm to room temperature while stirring under an atmosphere of N_2 for 18 h. At this time, the reaction was diluted with water (150 mL), which induced the precipitation of an orange solid. The solid was collected by filtration and recrystallized from the minimum amount of boiling ethyl acetate necessary for full dissolution. The orange crystals were collected *via* filtration and dried *in vacuo* to yield the title compound as orange crystals (1.82 g, 71%). ^{1}H NMR data was consistent with previous reports.[1]

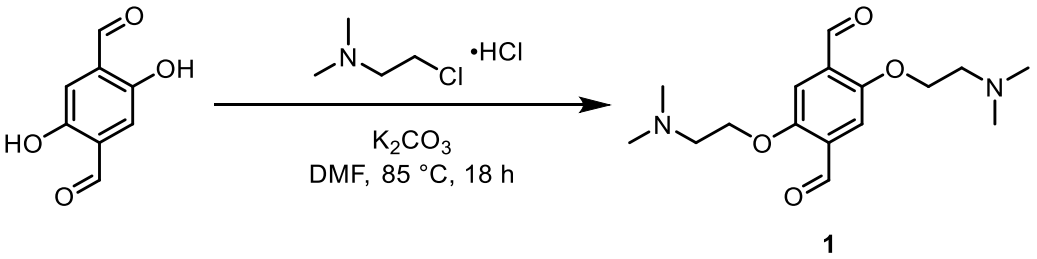

Synthesis of 1. A flame-dried 100 mL round bottom flask equipped with a magnetic stir bar was charged with 2,5-dihydroxy-1,4-dibenzaldehyde (500 mg, 3.00 mmol, 1.0 equiv), K_2CO_3 (2.50 g, 18.1 mmol, 6.0 equiv), and DMF (20 mL). Subsequently, 2-chloro-*N*,*N*-dimethylethylamine hydrochloride (1.08 g, 7.50 mmol, 2.5 equiv) was added and the reaction stirred under N_2 at 85 °C for 18 h. The reaction solution was then allowed to cool to room temperature. At this time, the solvent was removed from the reaction mixture with the aid of a rotary evaporator to yield the crude material as a brown solid. To this solid was added CH_2Cl_2 (80 mL) and aqueous NaOH (3 M, 50 mL). The organic layer was separated, and the aqueous layer extracted with additional CH_2Cl_2 (2 × 60 mL). The combined organic layers were washed with aqueous NaOH, dried over $MgSO_4$, and filtered before being concentrated under reduced pressure overnight to yield **1** as a brown solid (620 mg, 67%). ^{1}H NMR (500 MHz, $CDCl_3$) δ 10.51 (s, 2H), 7.46 (s, 2H), 4.20 (t, J = 5.5 Hz, 4H), 2.78 (t, J = 5.5 Hz, 4H), 2.34 (s, 12H). ^{13}C NMR (126 MHz, $CDCl_3$) δ 189.26, 155.16, 129.40, 111.97, 67.65, 58.14, 45.99. ESI HRMS *m/z* calculated for $[C_{16}H_{24}N_2O_4+H]^+$ 309.1814, found: 309.1809.

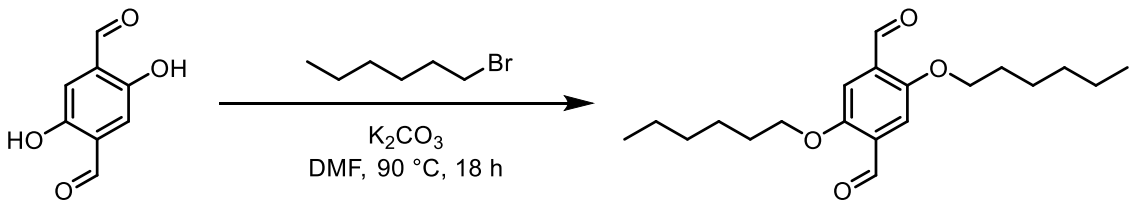

Synthesis of 2,5-dihexyloxy-1,4-dibenzaldehyde.[2] A flame-dried 100 mL round bottom flask equipped with a magnetic stir bar was charged with 2,5-dihydroxy-1,4-dibenzaldehyde (650 mg, 3.9 mmol, 1.0 equiv), K_2CO_3 (3240 mg, 23.5 mmol, 6.0 equiv), and DMF (30 mL). To this solution was added 1-bromohexane (3.3 mL, 23.6 mmol, 6.0 equiv) *via* syringe. The reaction solution was heated to 90 °C under an atmosphere of N_2 for 18 h. After allowing the reaction to cool to room temperature, water (60 mL) was added, and the reaction mixture extracted with ethyl acetate (3 × 50 mL). The combined organic layers were dried over $MgSO_4$, filtered, and concentrated with the aid of a rotary evaporator. The solids were subjected to column chromatography (SiO_2, 100% hexanes) to yield the title compound (974 mg, 74%) as yellow crystals. ^{1}H NMR data was consistent with previous reports.[2]

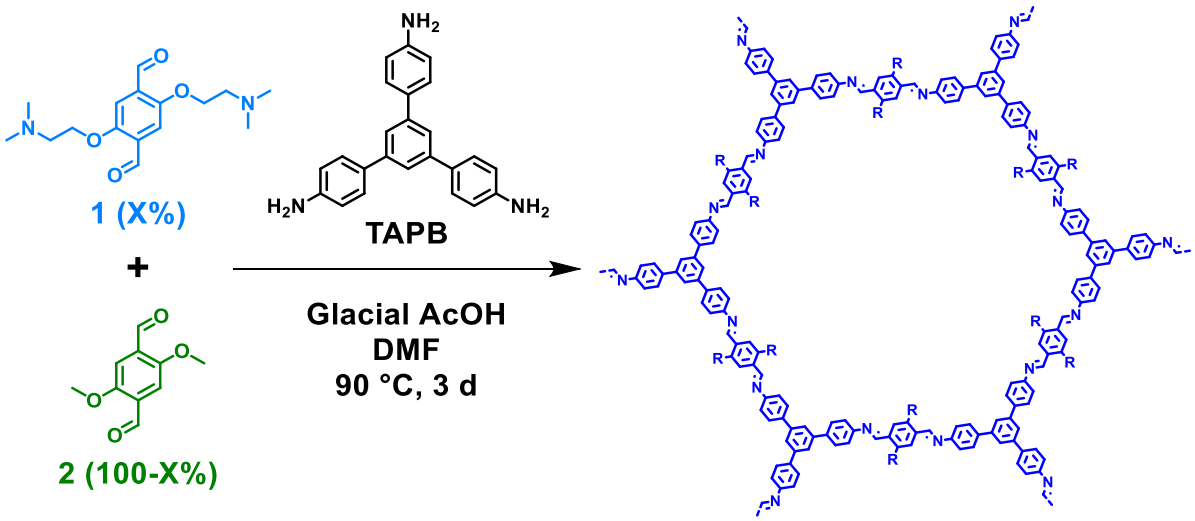

Synthesis of 100%[NR3]-2DP.[3] A 20 mL scintillation vial was charged with **1** (98.7 mg, 0.32 mmol, 1.5 equiv), TAPB (75 mg, 0.21 mmol, 1.0 equiv), and 13 mL DMF, then gently heated and sonicated until all components dissolved. Subsequently, glacial acetic acid (248 uL) was added *via* syringe and the reaction heated at 90 °C for 3 days. The reaction mixture was moved to a teabag and washed with a 5% triethylamine/methanol solution before washing with methanol in a Soxhlet extractor for 18 h. Afterwards, the solids were activated by supercritical CO_2 drying to yield 101.3 mg (62%) of product as yellow solids.

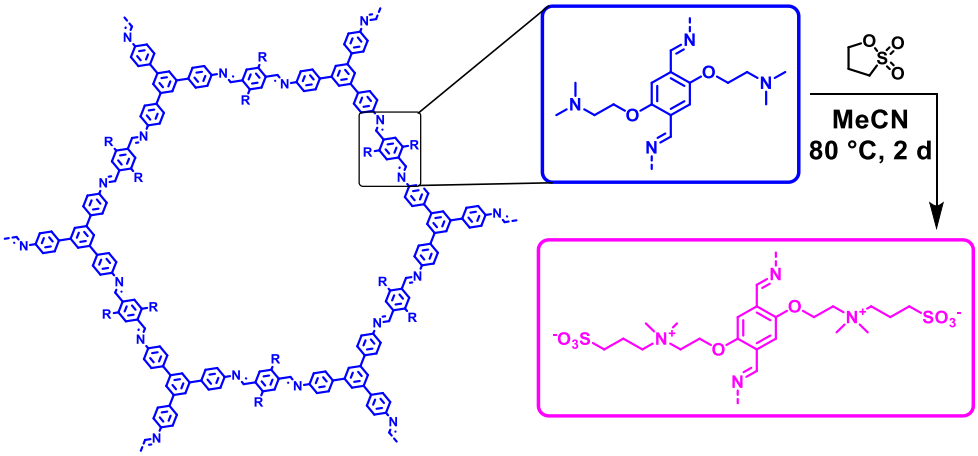

Converting 100%[NR$_3$]-2DP to zwitterionic 2DP. A 20 mL scintillation vial was charged with **100%[NR$_3$]-2DP** (35.0 mg, 0.069 mmol of linker, 0.138 mmol of dimethylamine groups) and 6 mL of acetonitrile. To this was added a solution of 1,3-propanesultone (16.9 mg, 0.138 mmol, 2.0 equiv relative to mmol of linker) in 1 mL of MeCN *via* syringe. The reaction mixture was left to heat, without stirring, at 80 °C for 2 days. The reaction mixture was moved to a teabag and rinsed with acetone before washing with acetone in a Soxhlet extractor for 18 h. Afterwards, the solids were activated by supercritical CO_2 drying to yield 49.0 mg (94%) of product as dark orange solids. The final zwitterion loading of the 2DP product was quantified through ^{1}H NMR digestion (see **Section C** for procedures and analysis of zwitterion loading).

Synthesis of Y$_1$%[NR$_3$]-C$_1$-2DPs. A similar procedure was followed as above, but at different molar ratios X%/(100-X)% of the two aldehyde components **1** and 2,5-dimethoxy-1,4-dibenzaldehyde (total moles of aldehydes equaled 1.5 times moles of TAPB). The dimethylamine loadings of the 2DP products were quantified through ^{1}H NMR digestion (see **Section C**). Isolated yields ranged from 37%-92% for the 2DPs examined.

Synthesis of Y$_2$%[NR$_3$]-Z$_1$-2DPs. A similar procedure was followed as above, but the mmol sultone added arose from the calculated dimethylamine loading (see Section C for a discussion on quantifying this). The final zwitterion loadings of the 2DP products were quantified through ^{1}H NMR digestion (see **Section C**). Isolated yields ranged from 91%-100% for the 2DPs examined.

Synthesis of Y$_1$%[NR$_3$]-C$_6$-2DPs. A similar procedure was followed as **Y$_1$%[NR$_3$]-C$_1$-2DP**s above, but using co-linker 2,5-dihexyloxy-1,4-dibenzaldehyde instead of 2,5-dimethoxy-1,4-dibenzaldehyde. Isolated yields ranged from 44%-80% for the 2DPs examined.

Synthesis of Y$_2$%[NR$_3$]-Z$_6$-2DPs. A similar procedure was followed as **Y$_2$%[NR$_3$]-Z$_1$-2DP**s above. Isolated yields ranged from 72%-100% for the 2DPs examined.

C. NMR Digestion Studies

General 2DP digestion procedure: this procedure was adapted from a previous report.[4] 1.5 mg of 2DP powder was added to a 4 mL vial along with 0.6 mL of DMSO-d_6 and 0.1 mL of DCl. This mixture was sonicated for 2 minutes and heated at 90 °C for 5 minutes to furnish clear yellow solutions and then submitted for ^{1}H NMR analysis with DMSO as the reference solvent.

The dimethylamine 2DPs were acid-digested to return aldehyde monomers in solution: a mixture of dimethylamine dialdehyde **1** and co-linker dialkoxy dialdehyde. The difference in integration values between proton resonances was used to calculate the percentage of dimethylamine groups relative to alkoxy groups, and thus the percentage of each linker present.

The zwitterionic 2DPs were acid-digested to return aldehyde monomers in solution: a mixture of dimethylamine dialdehyde **1**, zwitterionic dialdehyde, and co-linker dialkoxy dialdehyde. The difference in integration values between proton resonances of **1** and zwitterionic dialdehyde was used to calculate what percentage of dimethylamine groups were converted to zwitterions, and this percentage multiplied by the original dimethylamine loading gave the final zwitterion loading.

Example calculations are given below.

Example: Dimethylamine 2DPs

Sample calculation for the 9%[NR_3]-C_1-2DP: The signal at δ = 2.75 ppm corresponds to the methyl groups of dimethylamine, with an integration of 1.00 for 12 protons. The signal at δ = 3.76 ppm corresponds to the methyl groups of the methoxy chain, with an integration of 5.23 for 6 protons (in the hexyloxy 2DP series, instead the signal used is at δ = 0.70 ppm corresponding to 6 protons of the terminal methyl groups on the hexyl chains).

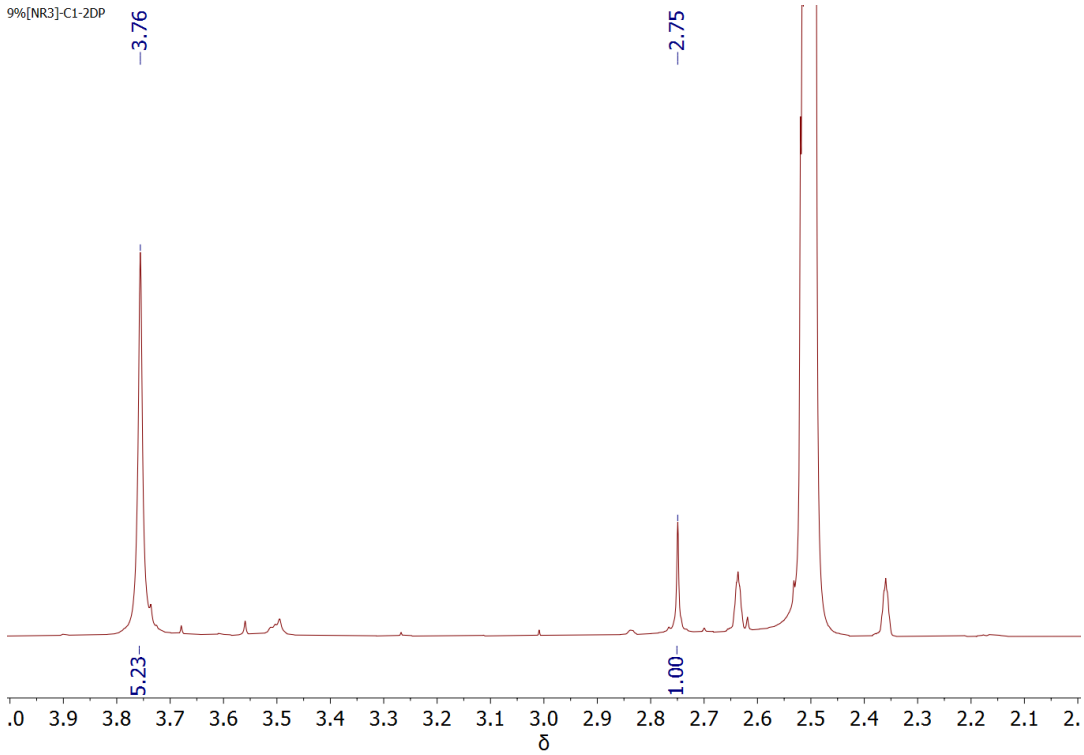

Figure S1. ^{1}H NMR spectrum of digested **9%[NR_3]-C_1-2DP**.

$$\frac{\dfrac{integration\ dimethylamine}{12\ protons\ dimethylamine}}{\dfrac{integration\ dimethylamine}{12\ protons\ dimethylamine}+\dfrac{integration\ alkoxy}{6\ protons\ alkoxy}} = \frac{\dfrac{1}{12}}{\dfrac{1}{12}+\dfrac{5.23}{6}} = 0.087 = 9\%$$

Yielding a final dimethylamine loading of 9%, meaning the remaining 91% of linkers are dimethoxy linkers.

Example: Zwitterionic 2DPs

Sample calculation for the 8%[NR$_3$]-Z$_1$-2DP: The signal at δ = 2.76 ppm corresponds to the methyl groups of unreacted dimethylamine, with an integration of 1.00 for 12 protons. The signal at δ = 3.09 ppm corresponds to the methyl groups of (reacted) zwitterion chains, with an integration of 11.69 for 12 protons. As the number of methyl groups is conserved throughout the reaction, thus the dimethylamine integration before the reaction = 1 + 11.69 = 12.69.

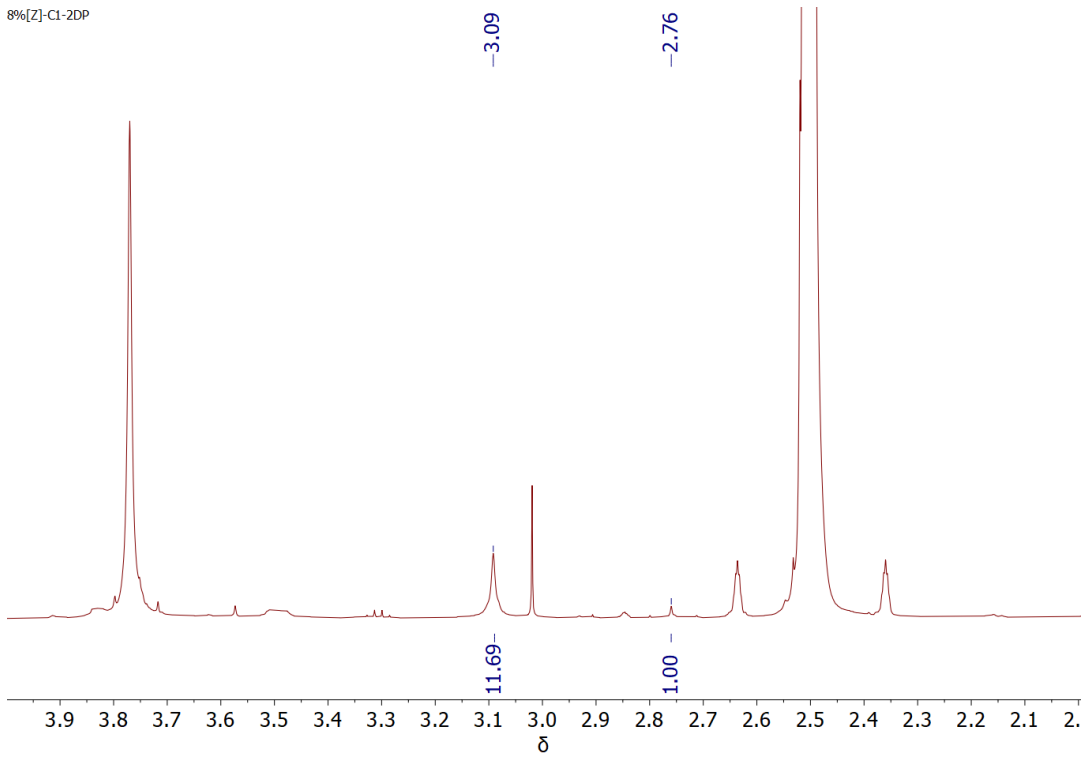

Figure S2. ^{1}H NMR spectrum of digested **8%[Z]-C$_1$-2DP**.

$$Conversion = 1 - \frac{Dimethylamine\ integration\ after\ reaction}{Dimethylamine\ integration\ before\ reaction} = 1 - \frac{1}{12.69} = 92\%$$

Thus, 92% of the dimethylamine groups were converted to zwitterionic groups.

With a conversion percentage known, the final zwitterion loading can be calculated as follows.

$$Final\ loading = initial\ loading \times conversion\ rate\ (\%)$$

$$Final\ loading = 9\% \times 0.92 = 8\%$$

Yielding a final zwitterion loading of 8% in this 2DP. The same procedure is applied for the zwitterionic hexyloxy 2DPs.

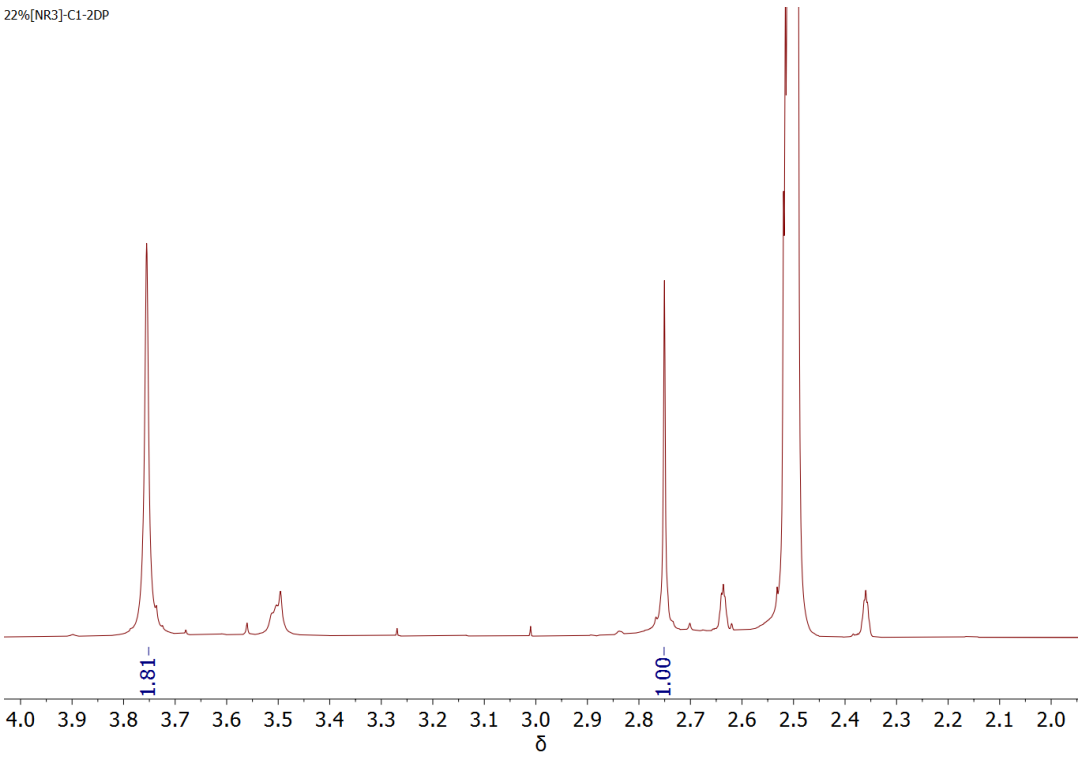

Figure S3. ^{1}H NMR spectrum of digested **22%[NR$_3$]-C$_1$-2DP**.

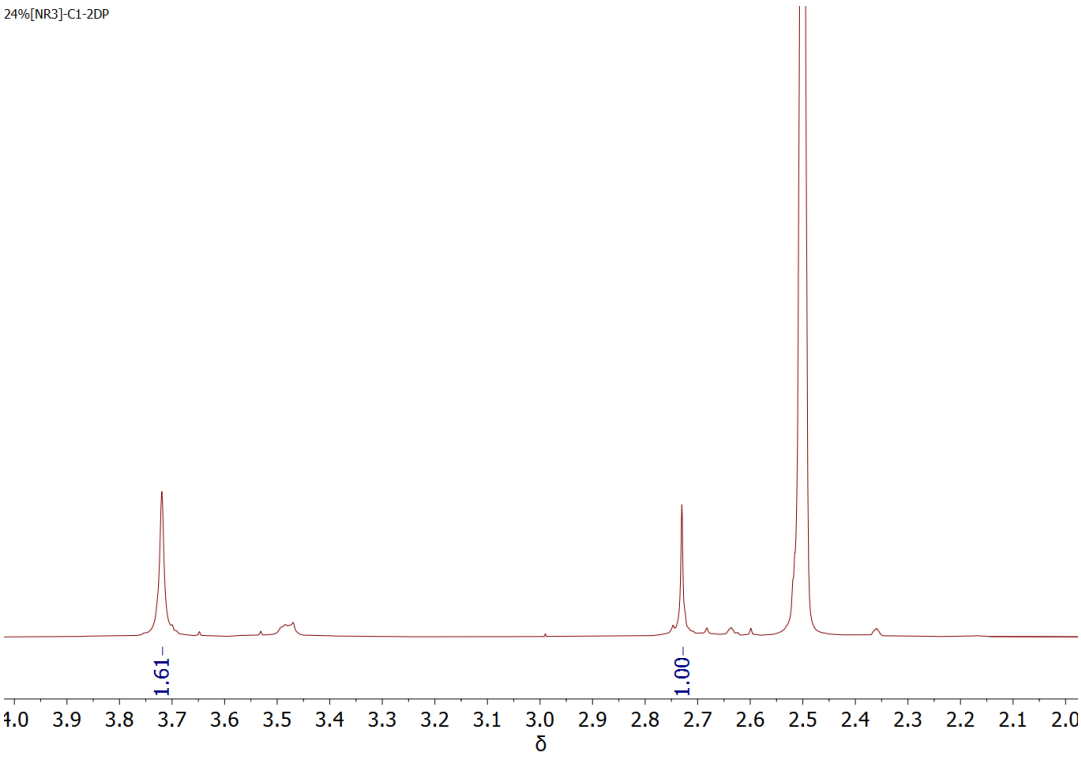

Figure S4. ^{1}H NMR spectrum of digested **24%[NR$_3$]-C$_1$-2DP**.

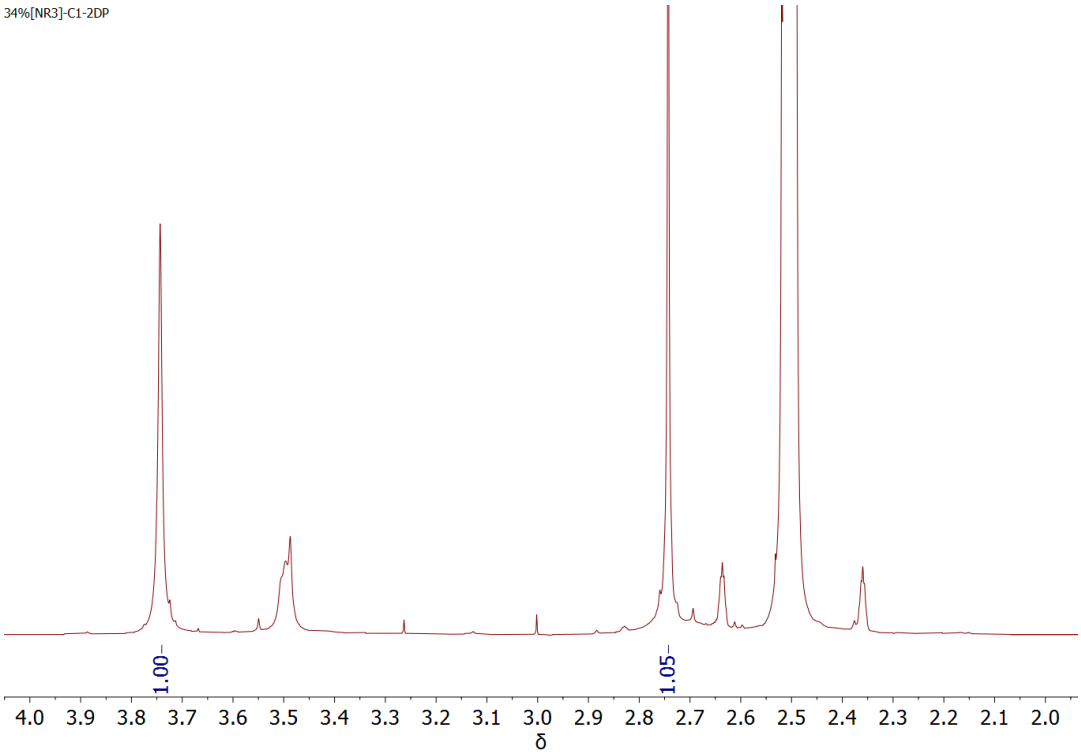

Figure S5. ^{1}H NMR spectrum of digested **34%[NR$_3$]-C$_1$-2DP**.

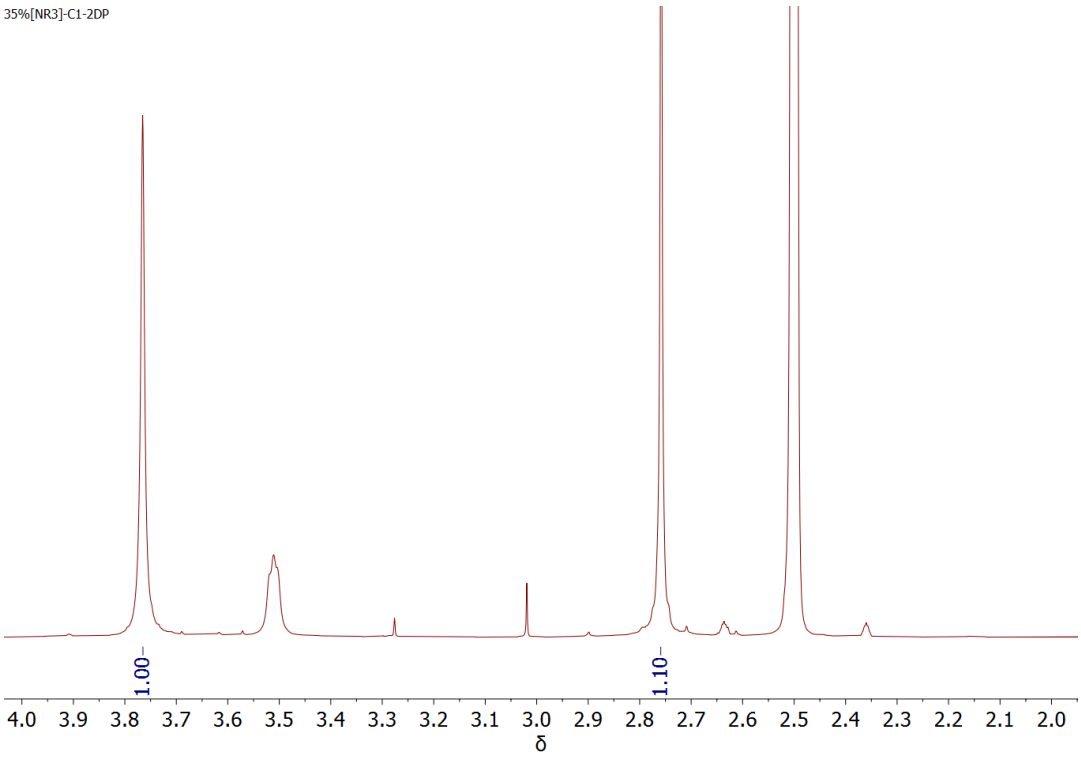

Figure S6. ^{1}H NMR spectrum of digested **35%[NR$_3$]-C$_1$-2DP**.

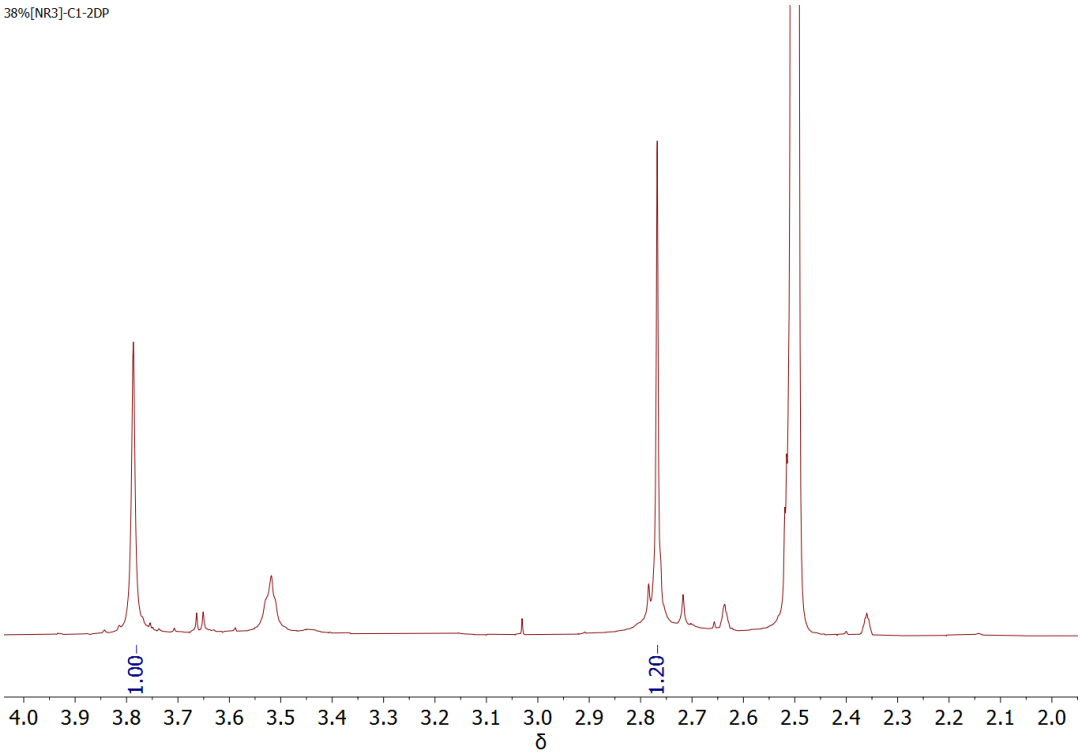

Figure S7. ^{1}H NMR spectrum of digested **38%[NR$_3$]-C$_1$-2DP**.

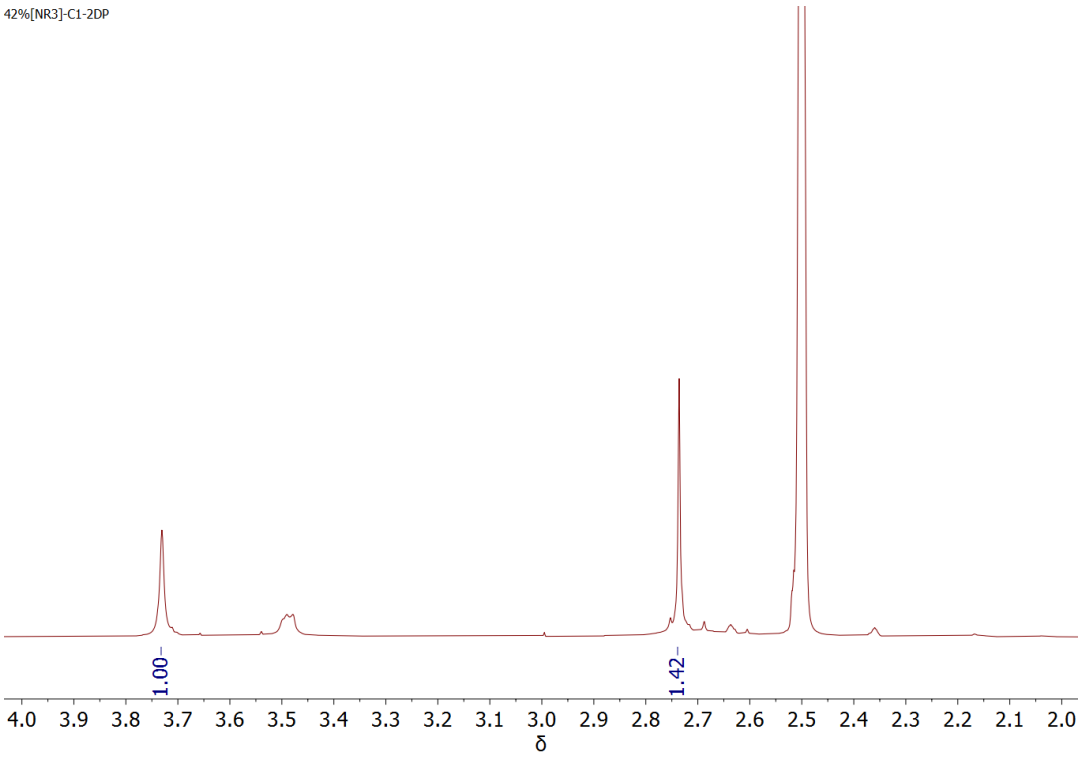

Figure S8. ^{1}H NMR spectrum of digested **42%[NR$_3$]-C$_1$-2DP**.

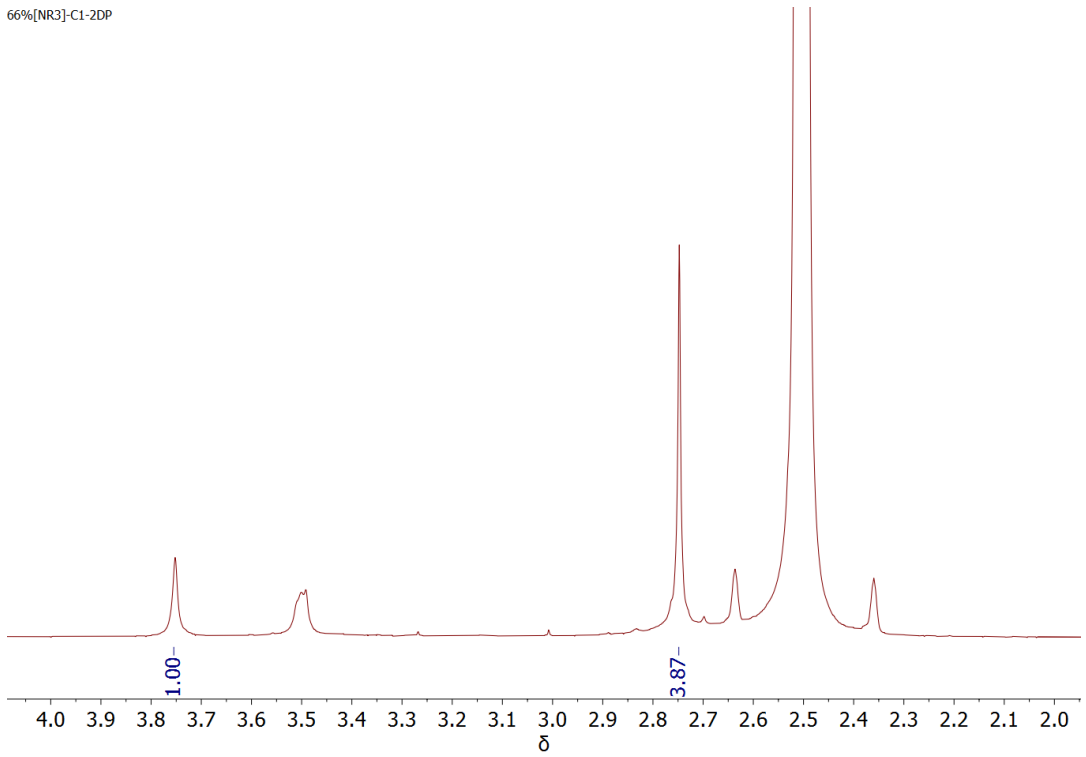

Figure S9. ^{1}H NMR spectrum of digested **66%[NR$_3$]-C$_1$-2DP**.

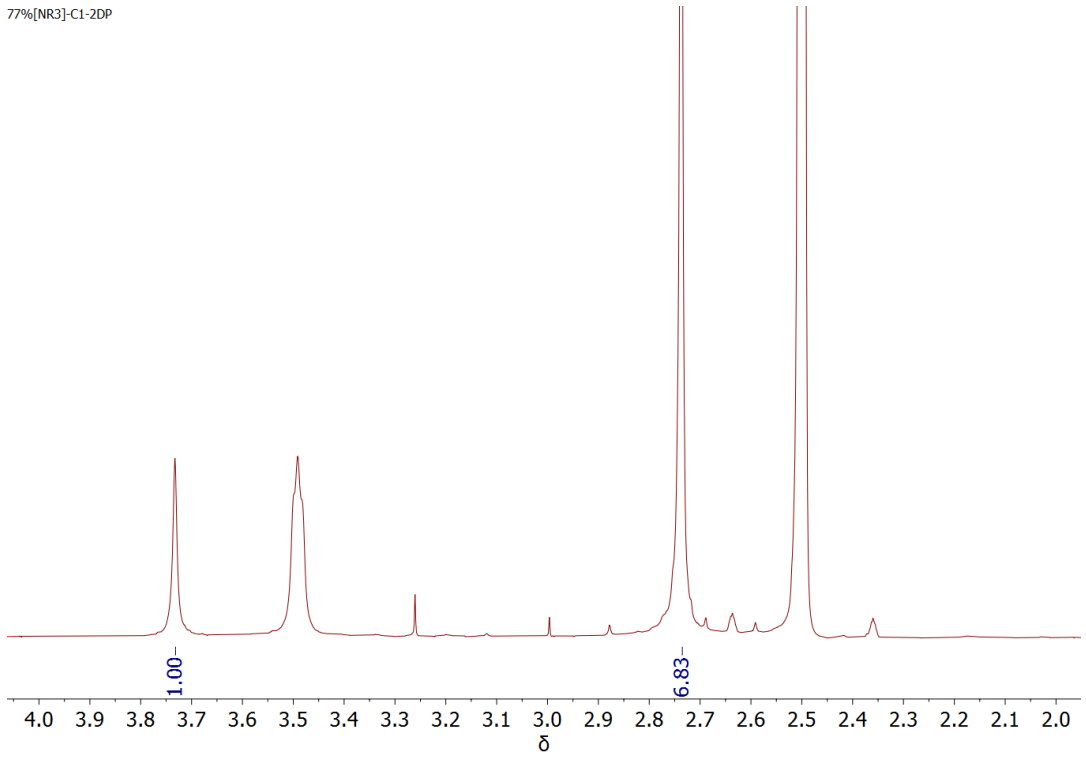

Figure S10. ^{1}H NMR spectrum of digested **77%[NR$_3$]-C$_1$-2DP**.

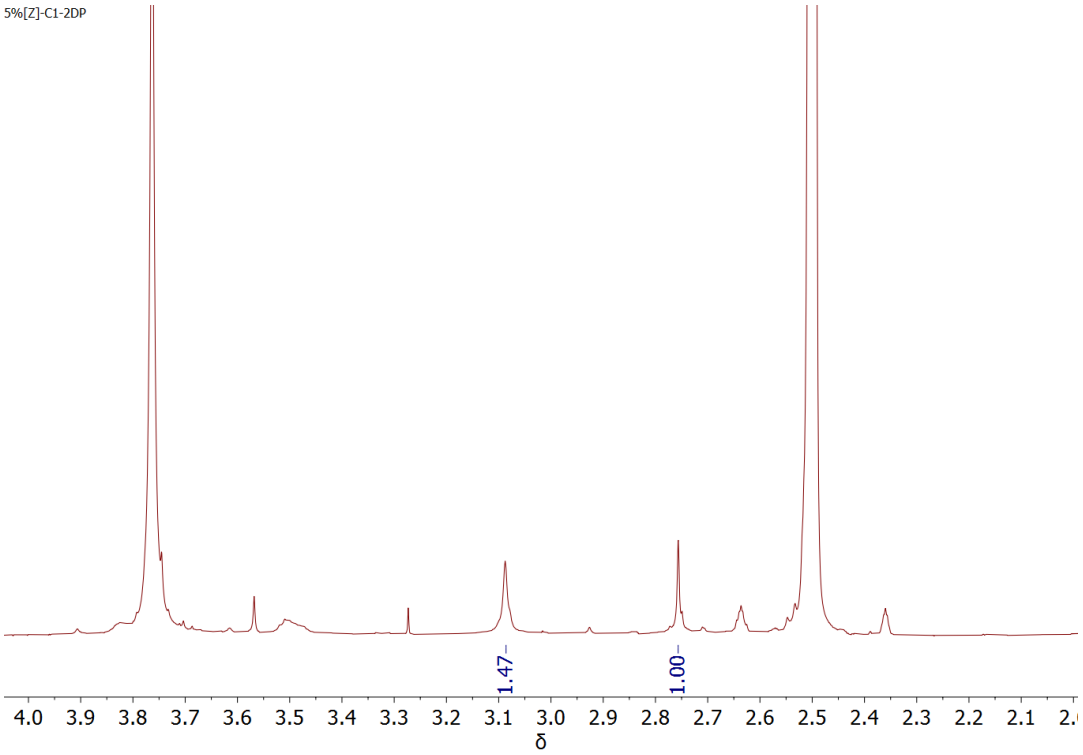

Figure S11. ^{1}H NMR spectrum of digested **5%[Z]-C$_1$-2DP**.

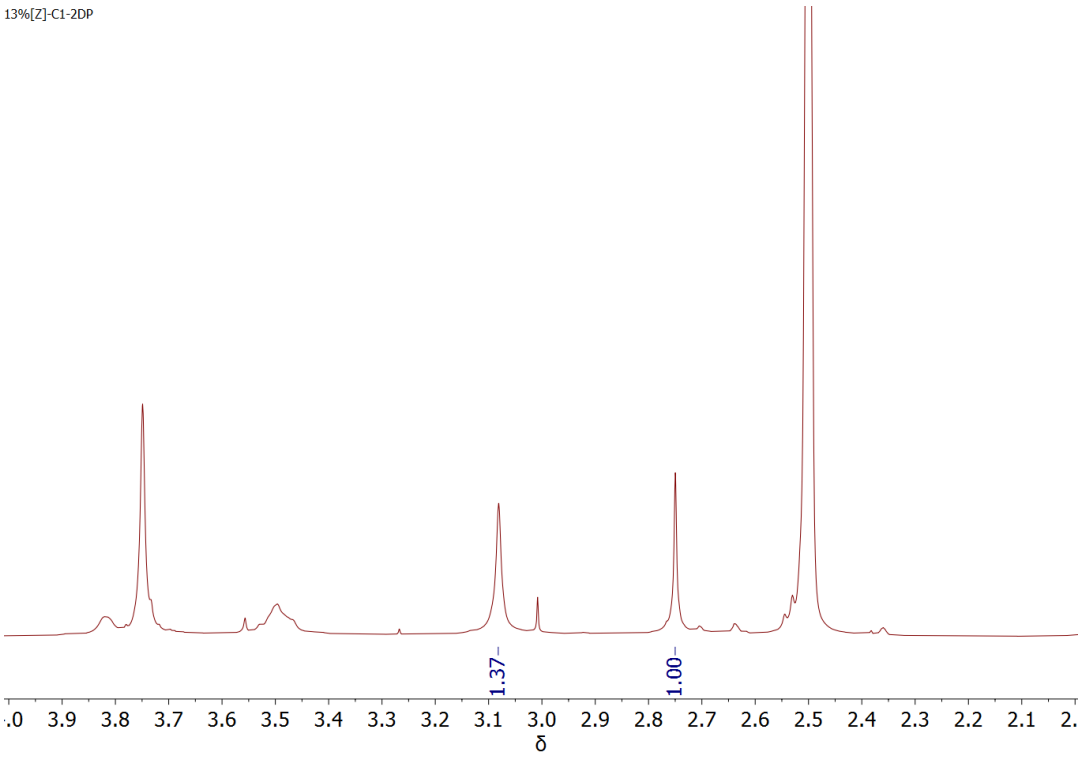

Figure S12. ^{1}H NMR spectrum of digested **13%[Z]-C$_1$-2DP**.

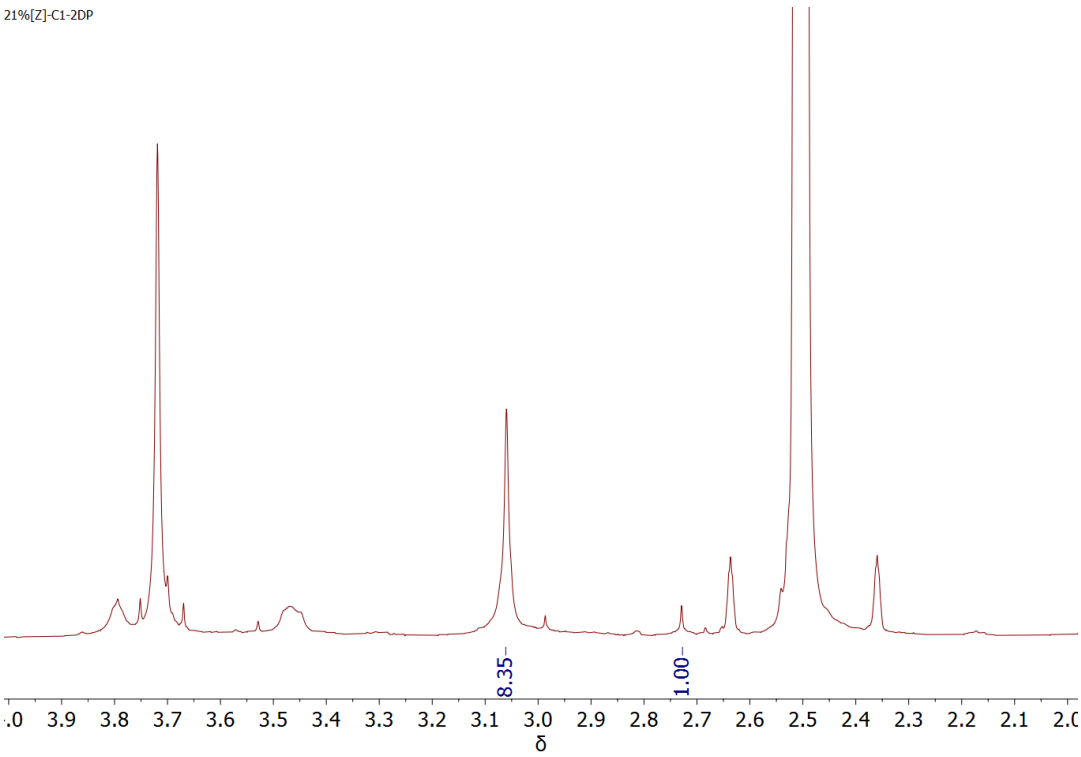

Figure S13. ^{1}H NMR spectrum of digested **21%[Z]-C$_1$-2DP**.

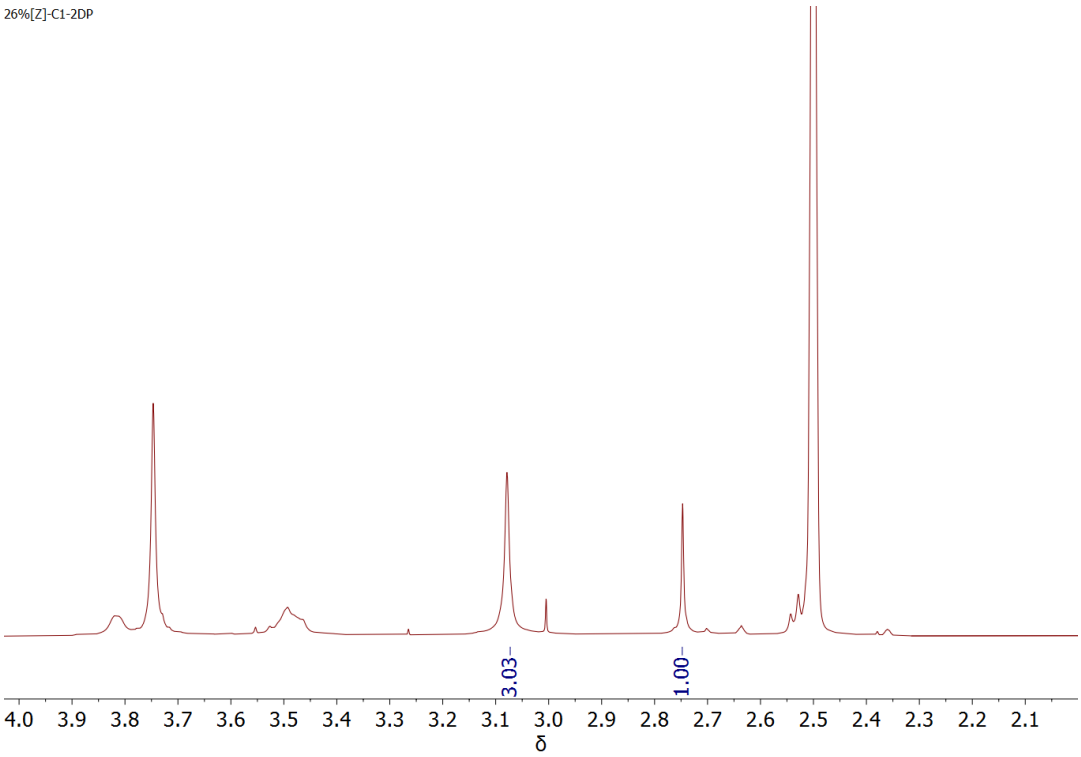

Figure S14. ^{1}H NMR spectrum of digested **26%[Z]-C$_1$-2DP**.

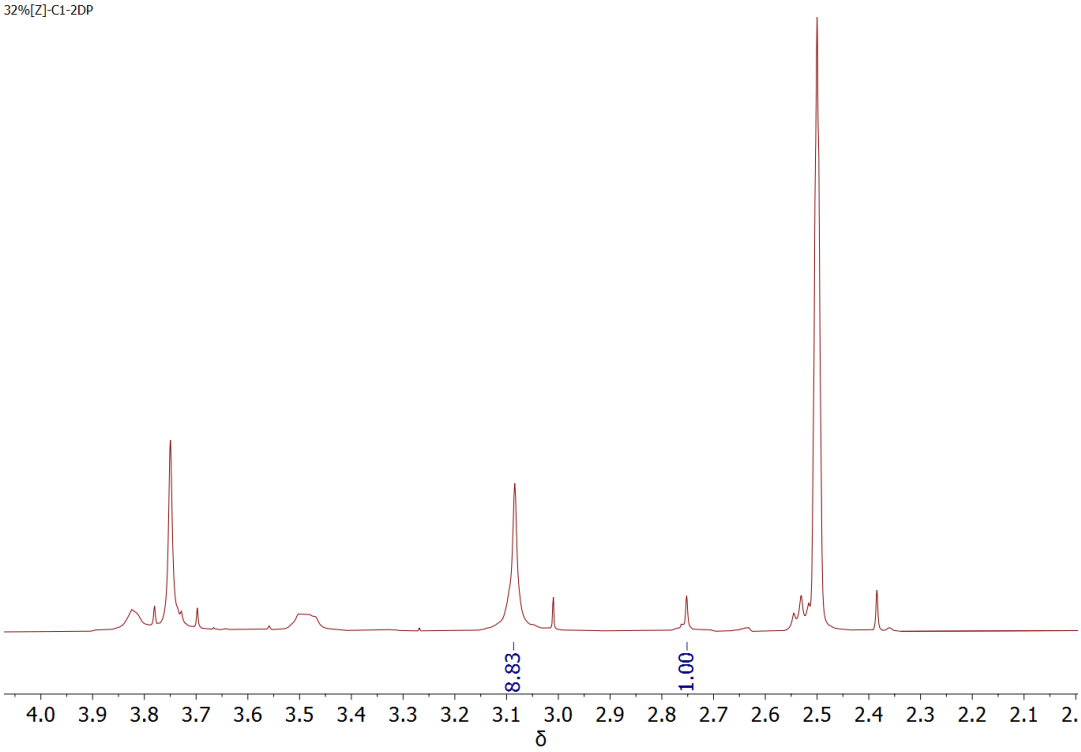

Figure S15. ^{1}H NMR spectrum of digested **32%[Z]-C$_1$-2DP**.

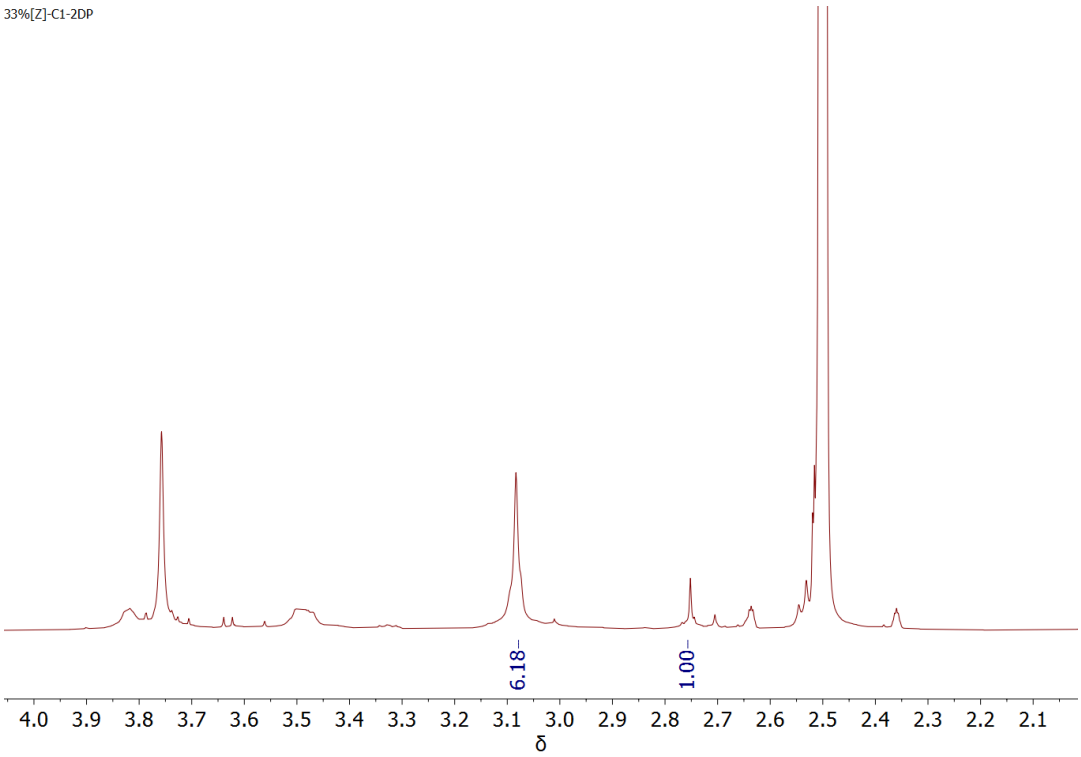

Figure S16. ^{1}H NMR spectrum of digested **33%[Z]-C$_1$-2DP**.

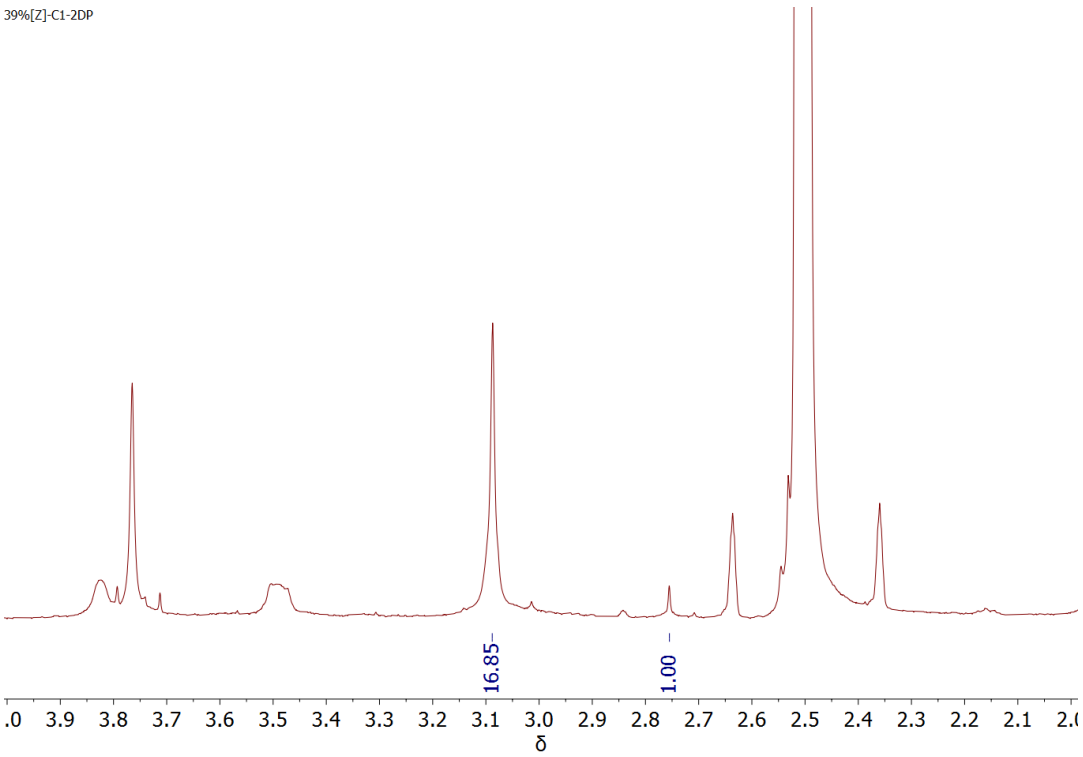

Figure S17. ^{1}H NMR spectrum of digested **39%[Z]-C$_1$-2DP**.

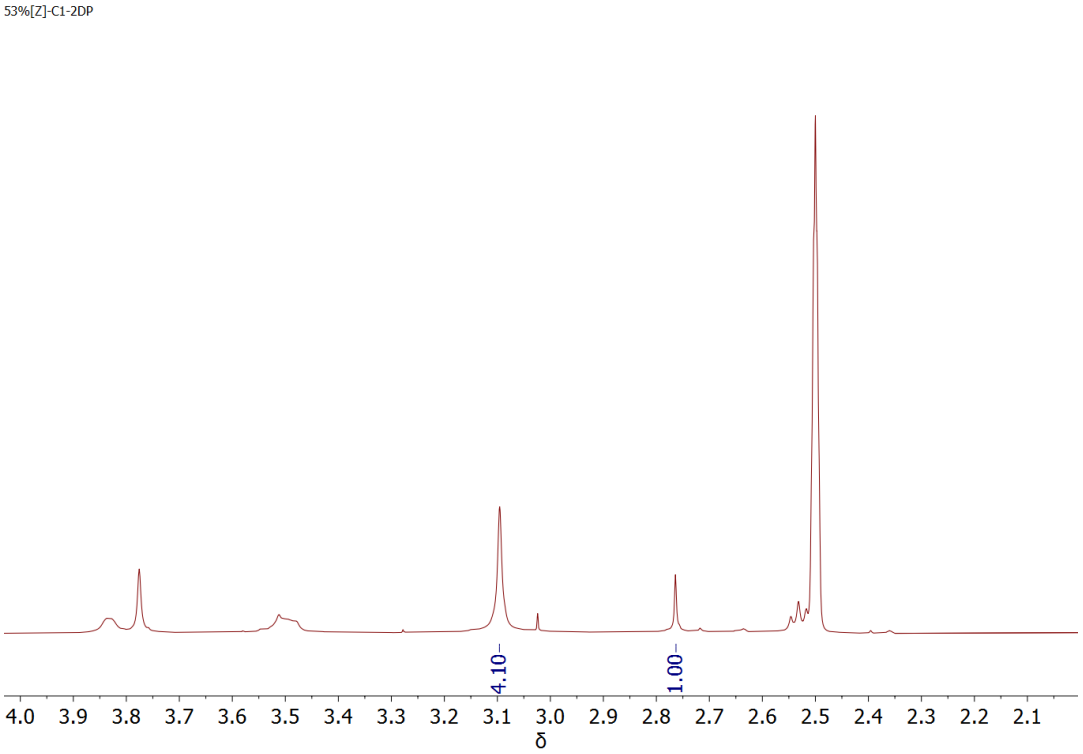

Figure S18. ^{1}H NMR spectrum of digested **53%[Z]-C$_1$-2DP**.

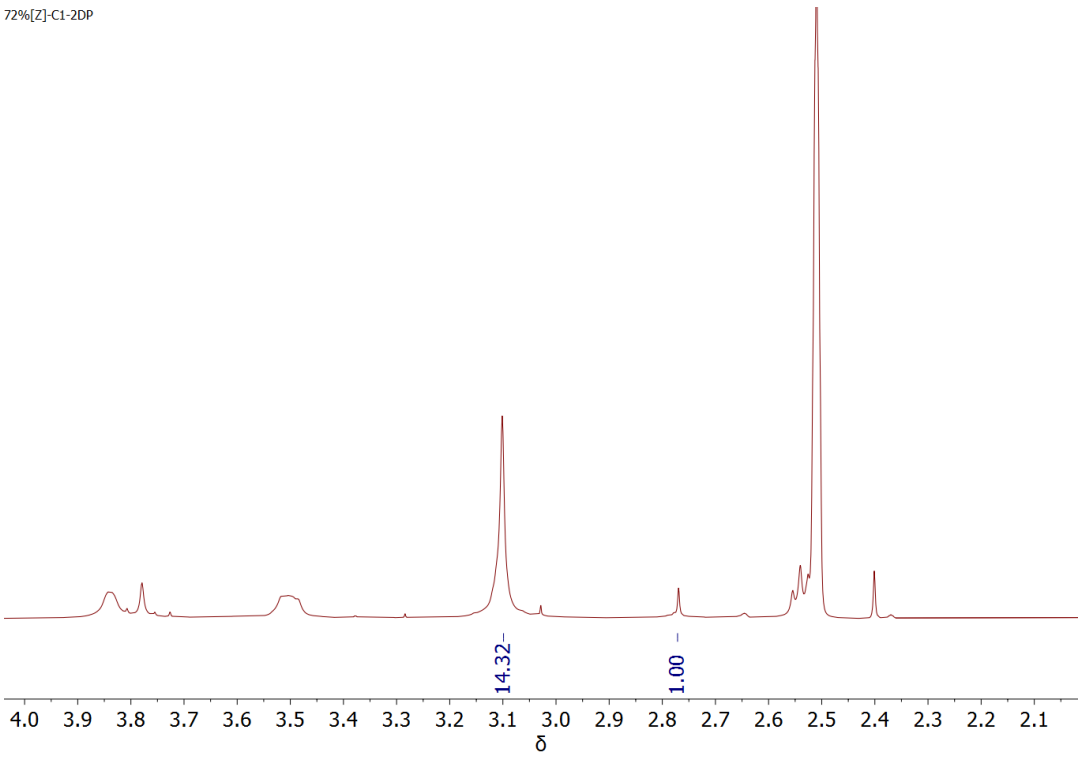

Figure S19. ^{1}H NMR spectrum of digested **72%[Z]-C$_1$-2DP**.

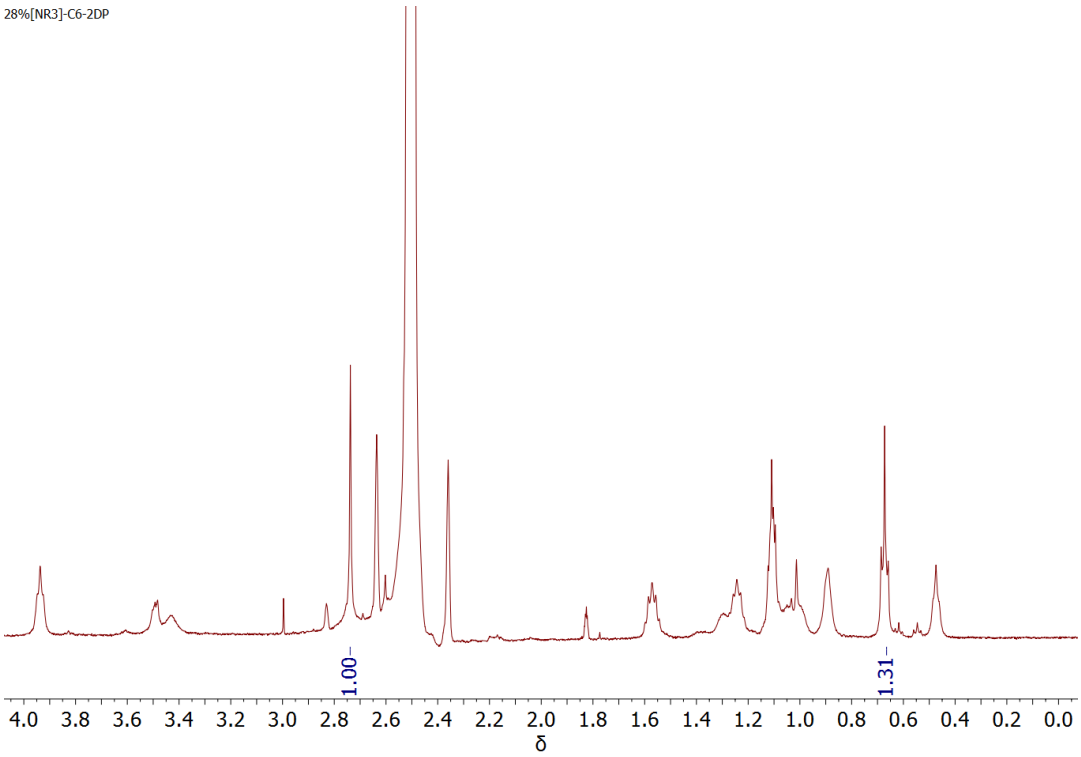

Figure S20. ^{1}H NMR spectrum of digested **28%[NR$_3$]-C$_6$-2DP**.

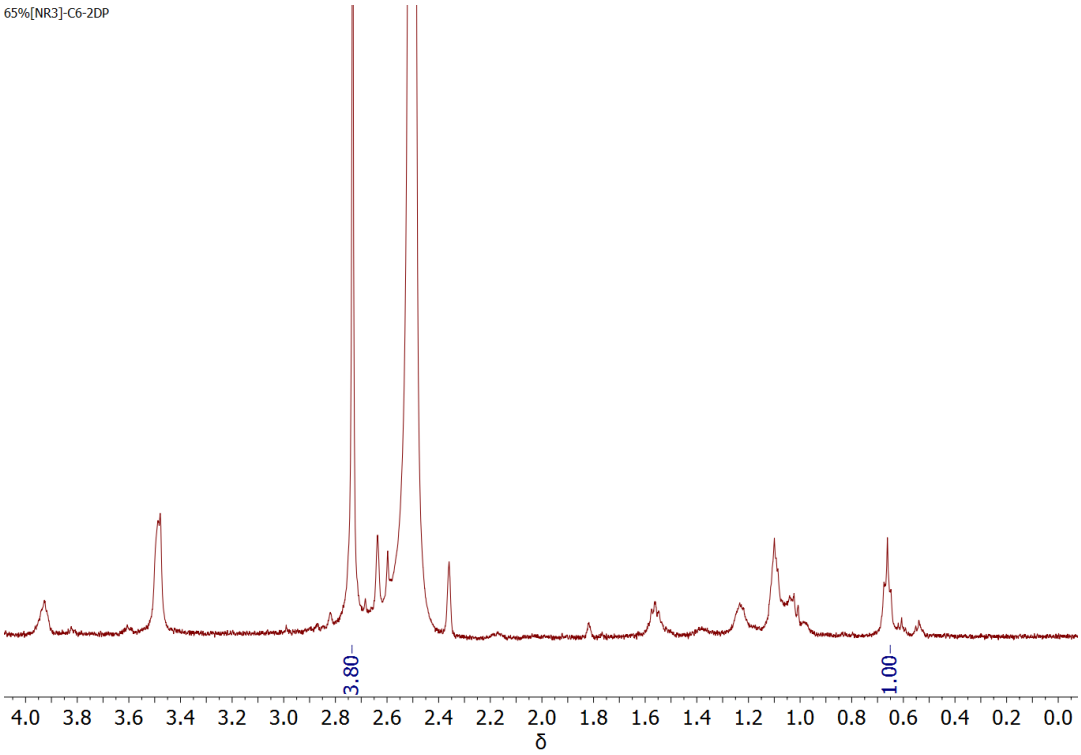

Figure S21. ^{1}H NMR spectrum of digested **65%[NR$_3$]-C$_6$-2DP**.

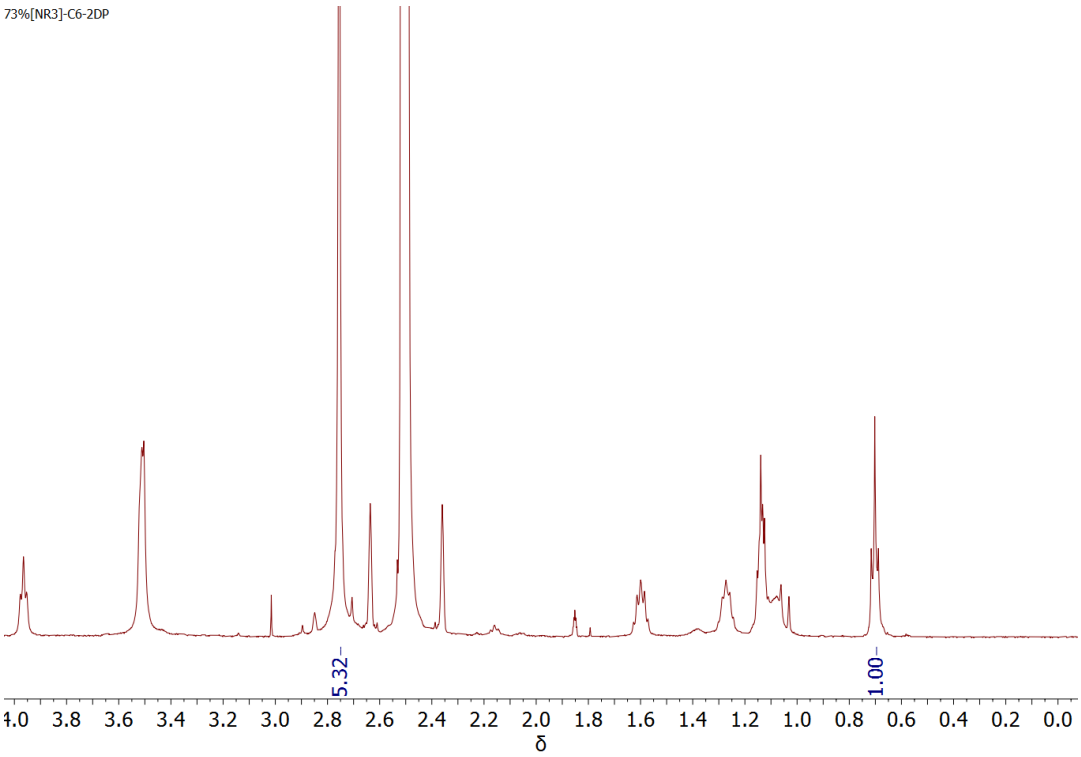

Figure S22. ^{1}H NMR spectrum of digested **73%[NR$_3$]-C$_6$-2DP**.

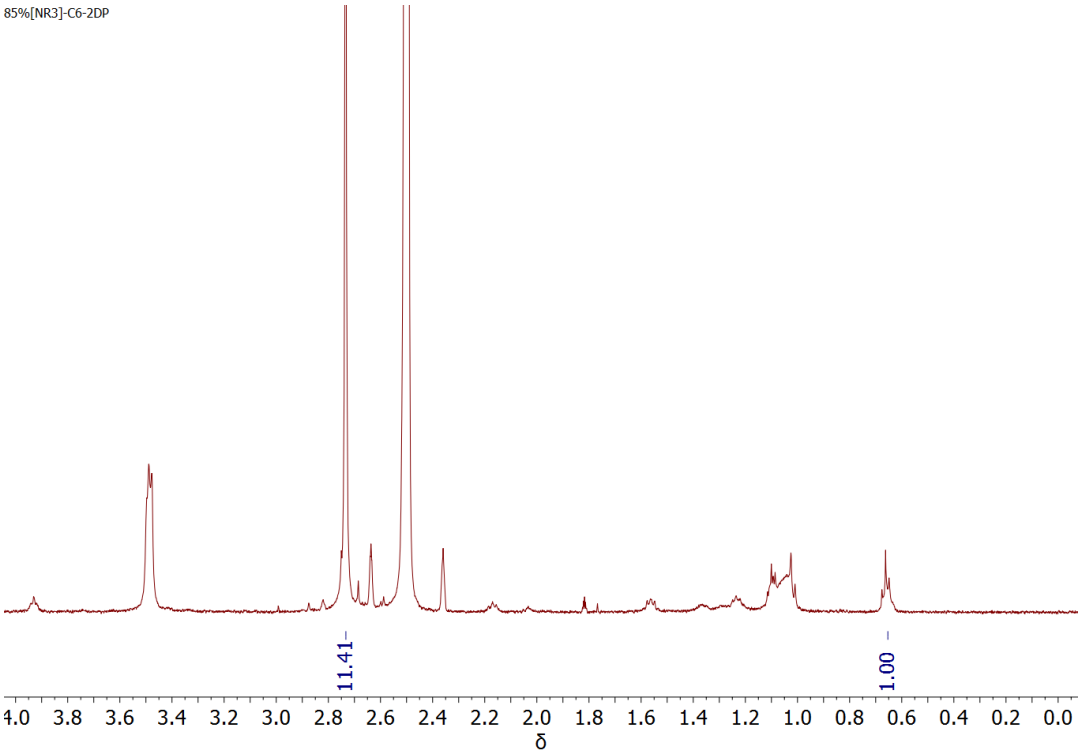

Figure S23. ^{1}H NMR spectrum of digested **85%[NR$_3$]-C$_6$-2DP**.

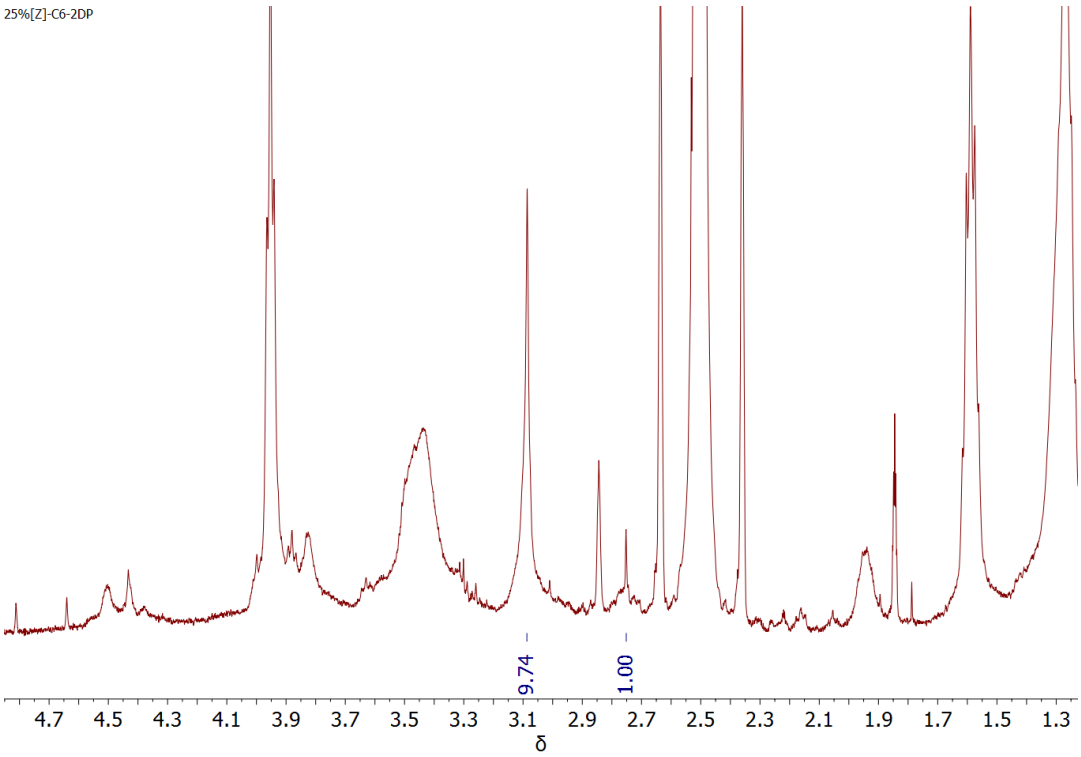

Figure S24. ^{1}H NMR spectrum of digested **25%[Z]-C$_6$-2DP**.

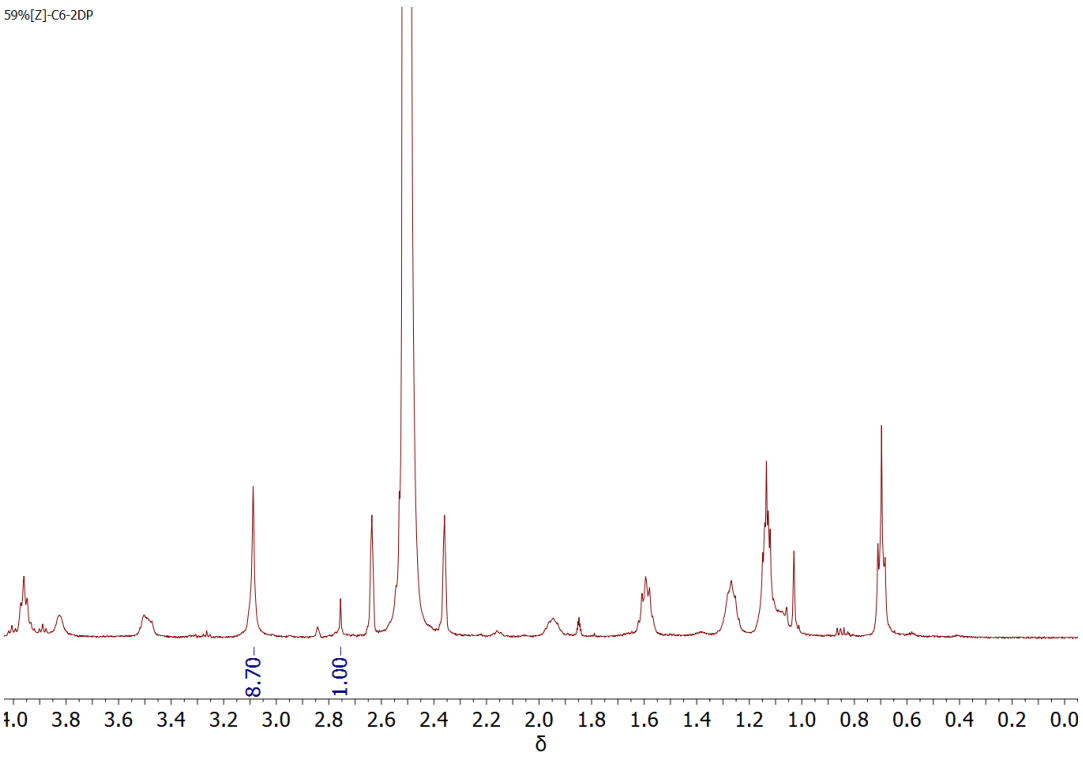

Figure S25. ^{1}H NMR spectrum of digested **59%[Z]-C$_6$-2DP**.

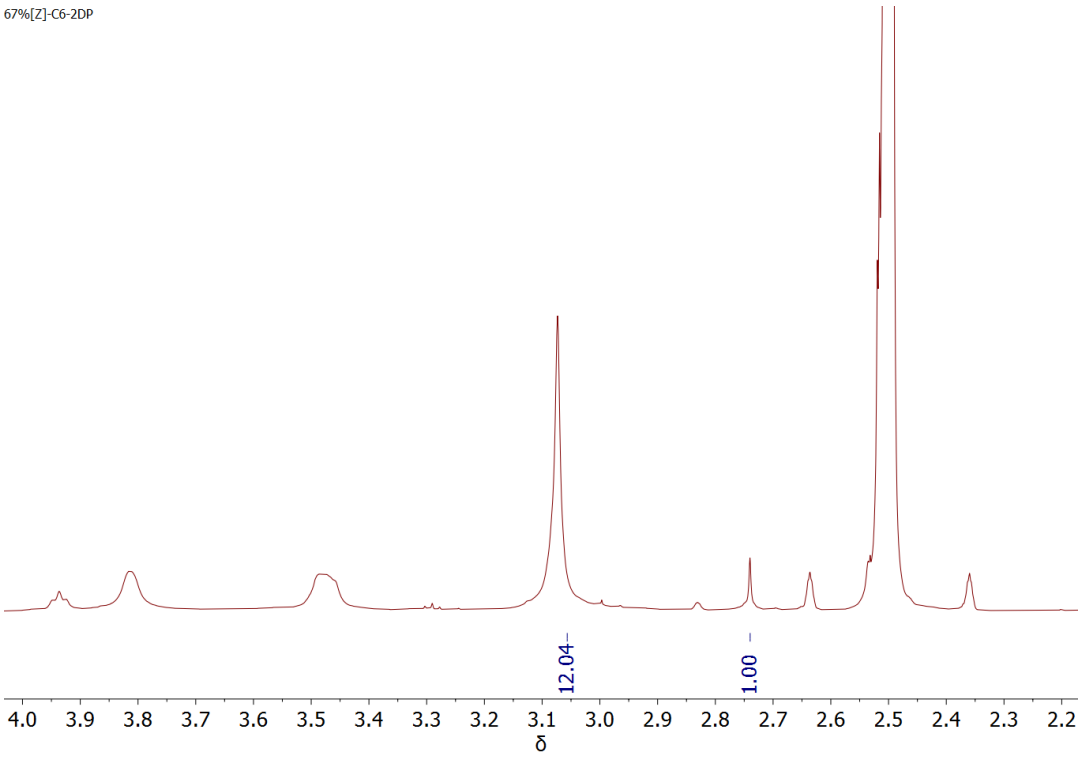

Figure S26. ^{1}H NMR spectrum of digested **67%[Z]-C$_6$-2DP**.

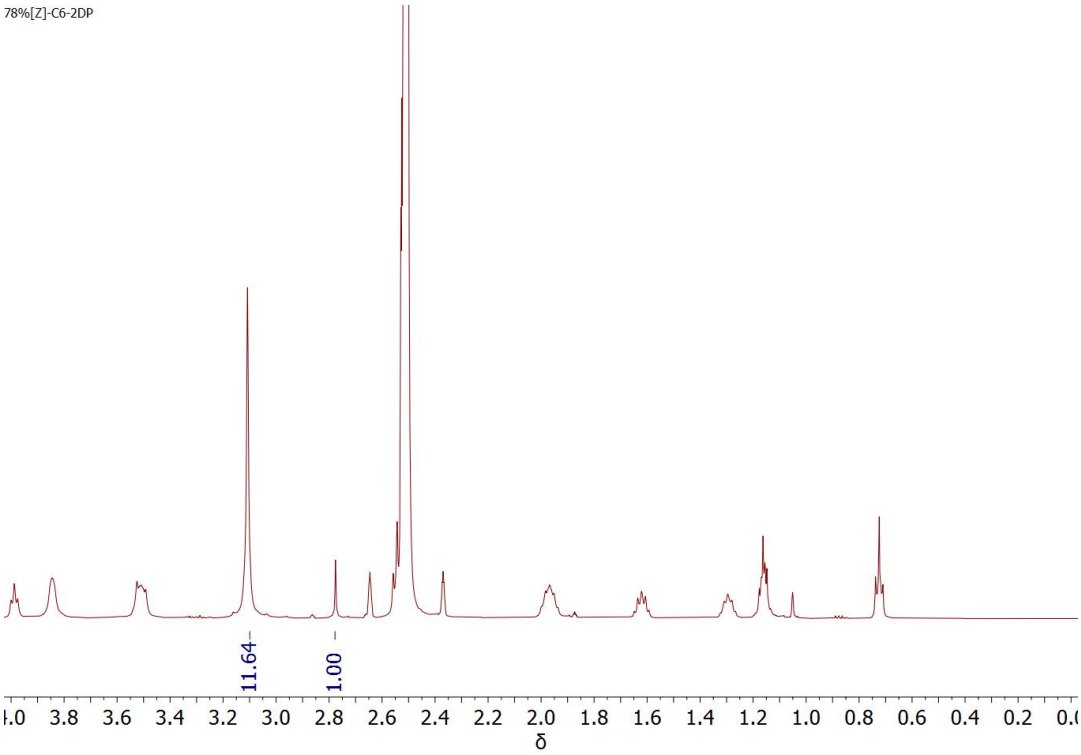

Figure S27. ^{1}H NMR spectrum of digested **78%[Z]-C$_6$-2DP**.

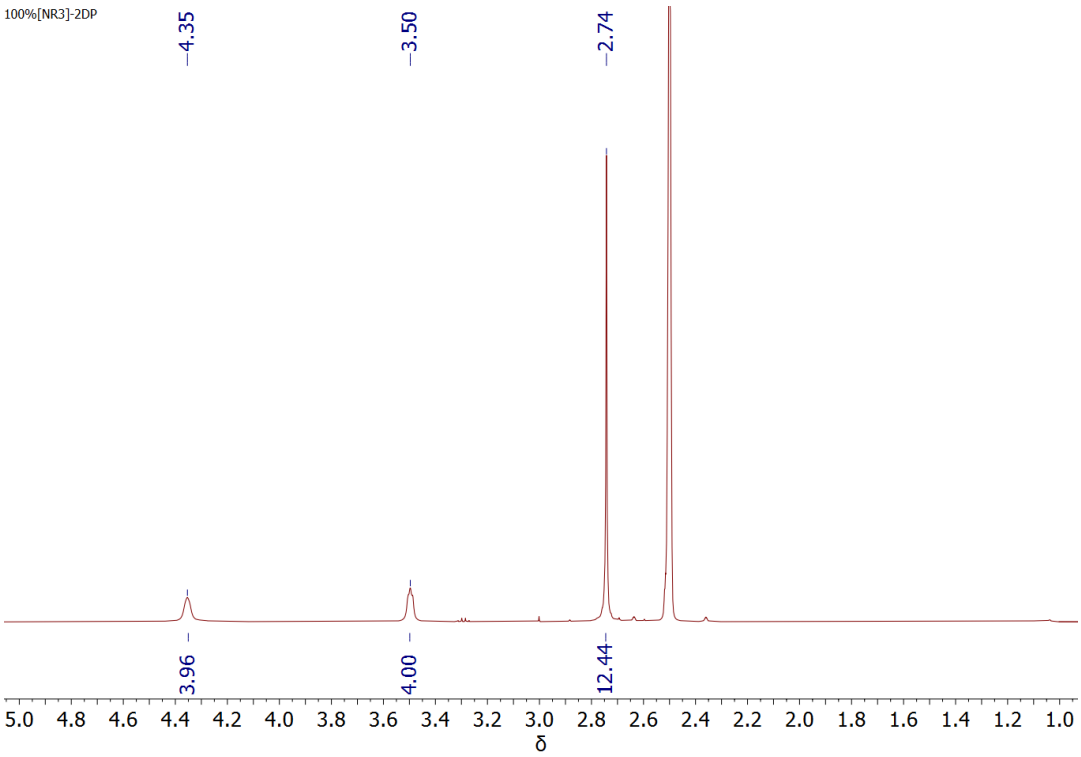

Figure S28. ^{1}H NMR spectrum of digested **100%[NR$_3$]-2DP**.

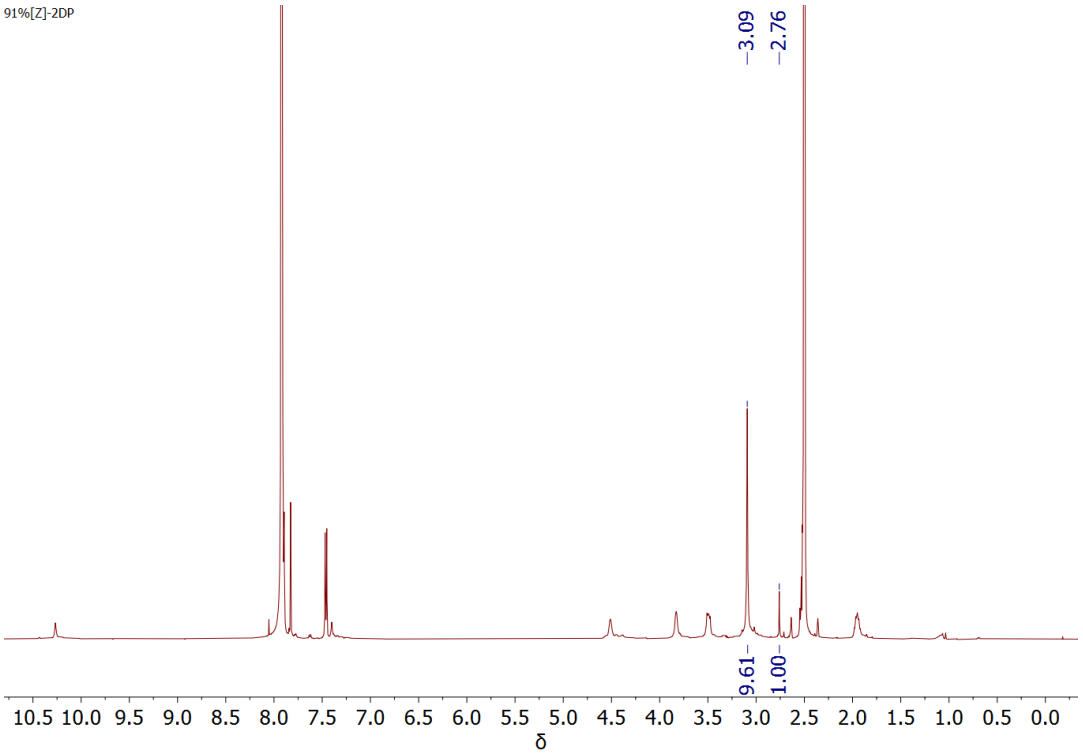

Figure S29. ^{1}H NMR spectrum of digested **91%[Z]-2DP**, originating from **100%[NR$_3$]-2DP**.

Table S1. Zwitterion-forming reaction conversions of 2DPs.

Co-linker	Dimethylamine Loading %	Conversion	Final Zwitterion Loading %
-	100	91%	91
C_1	9	60%	5
	9	92%	8
	22	58%	13
	24	89%	21
	34	75%	26
	35	90%	32
	38	86%	33
	42	94%	39
	66	80%	53
	77	93%	72
C_6	28	91%	25
	65	90%	59
	73	92%	67
	85	92%	78

D. PXRD and Nitrogen Porosimetry Data

PXRD Data

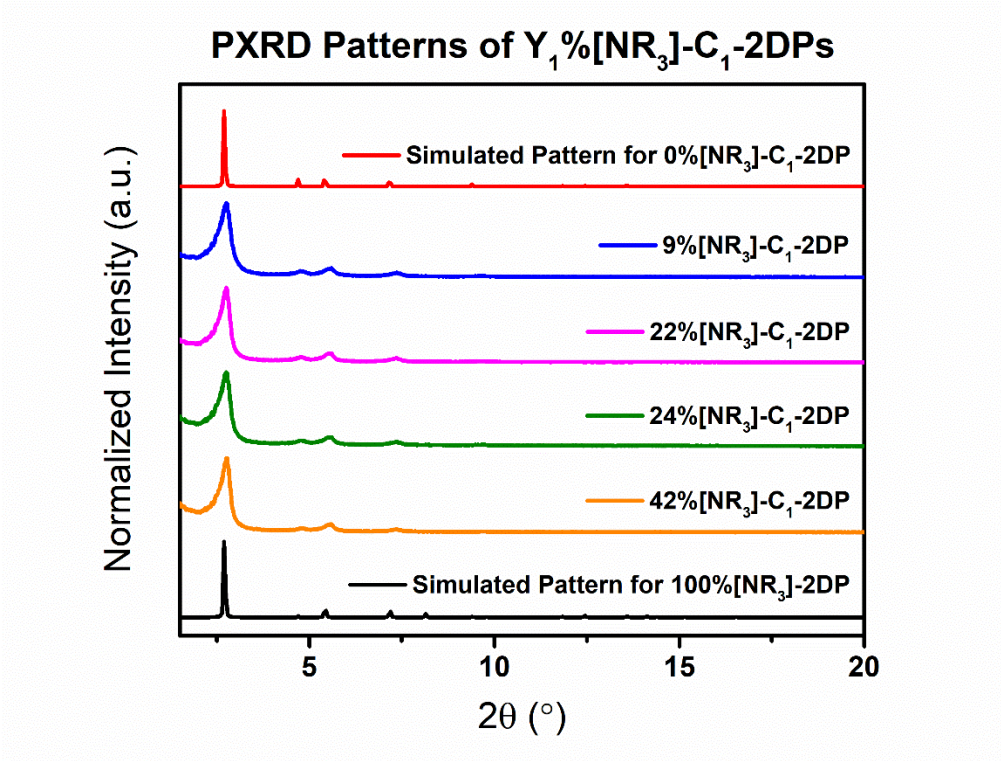

Figure S30. PXRD Patterns of **Y_1%[NR_3]-C_1-2DP**s before reactions with 1,3-propane sultone, along with simulated PXRD patterns of **0%[NR_3]-C_1-2DP** (a 2DP made with entirely C_1 linkers) and **100%[NR_3]-2DP**, calculated from Materials Studio. Predictions from Materials Studio describe hexagonal-pore **100%[NR_3]-2DP** forming as an eclipsed lattice stack with hexagonal unit cell dimensions of $a = b = 37.6$ Å and $c = 3.9$ Å.

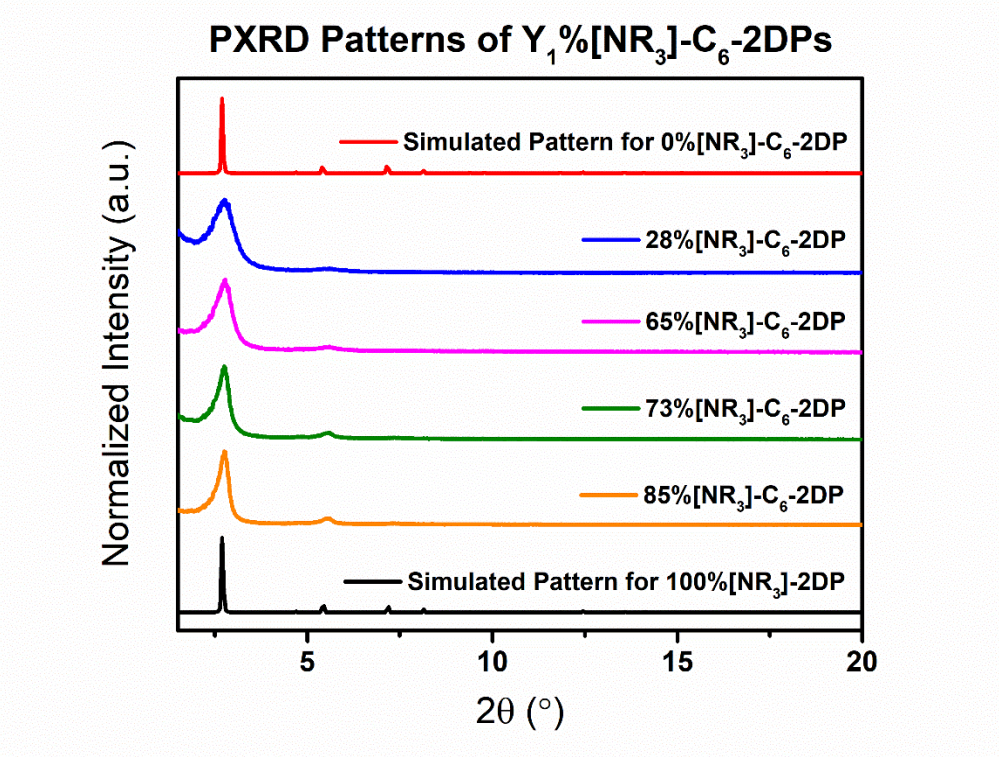

Figure S31. PXRD Patterns of **Y_1%[NR_3]-C_6-2DP**s before reactions with 1,3-propane sultone, along with simulated PXRD patterns of **0%[NR_3]-C_6-2DP** (a 2DP made with entirely C_6 linkers) and **100%[NR_3]-2DP**, calculated from Materials Studio. Predictions from Materials Studio describe hexagonal-pore **100%[NR_3]-2DP** forming as an eclipsed lattice stack with hexagonal unit cell dimensions of $a = b = 37.6$ Å and $c = 3.9$ Å.

Nitrogen Sorption Isotherms

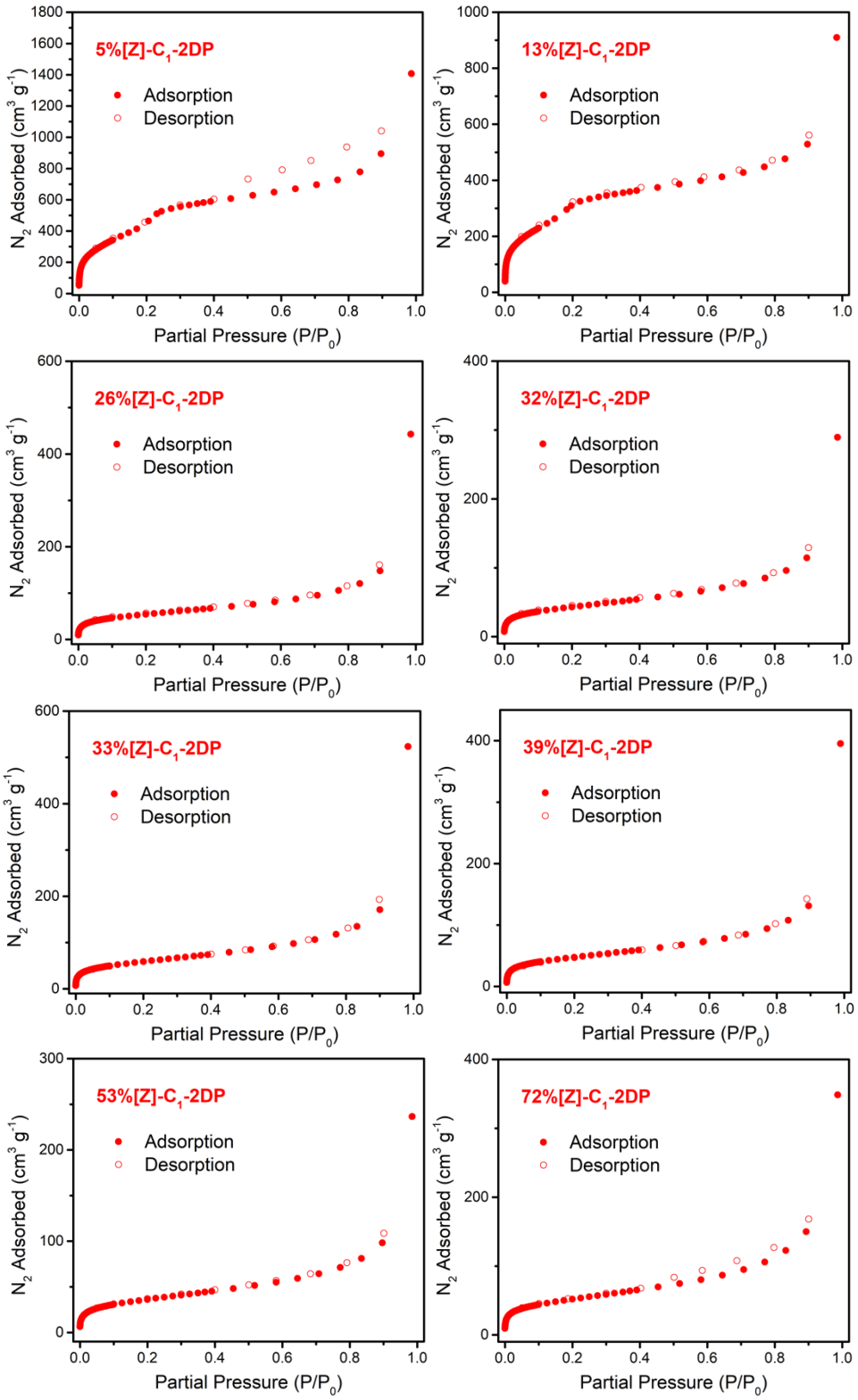

Figure S32. Nitrogen sorption isotherms for **Y_2%[Z]-C_1-2DP**s.

BET Plots for Surface Area Calculations

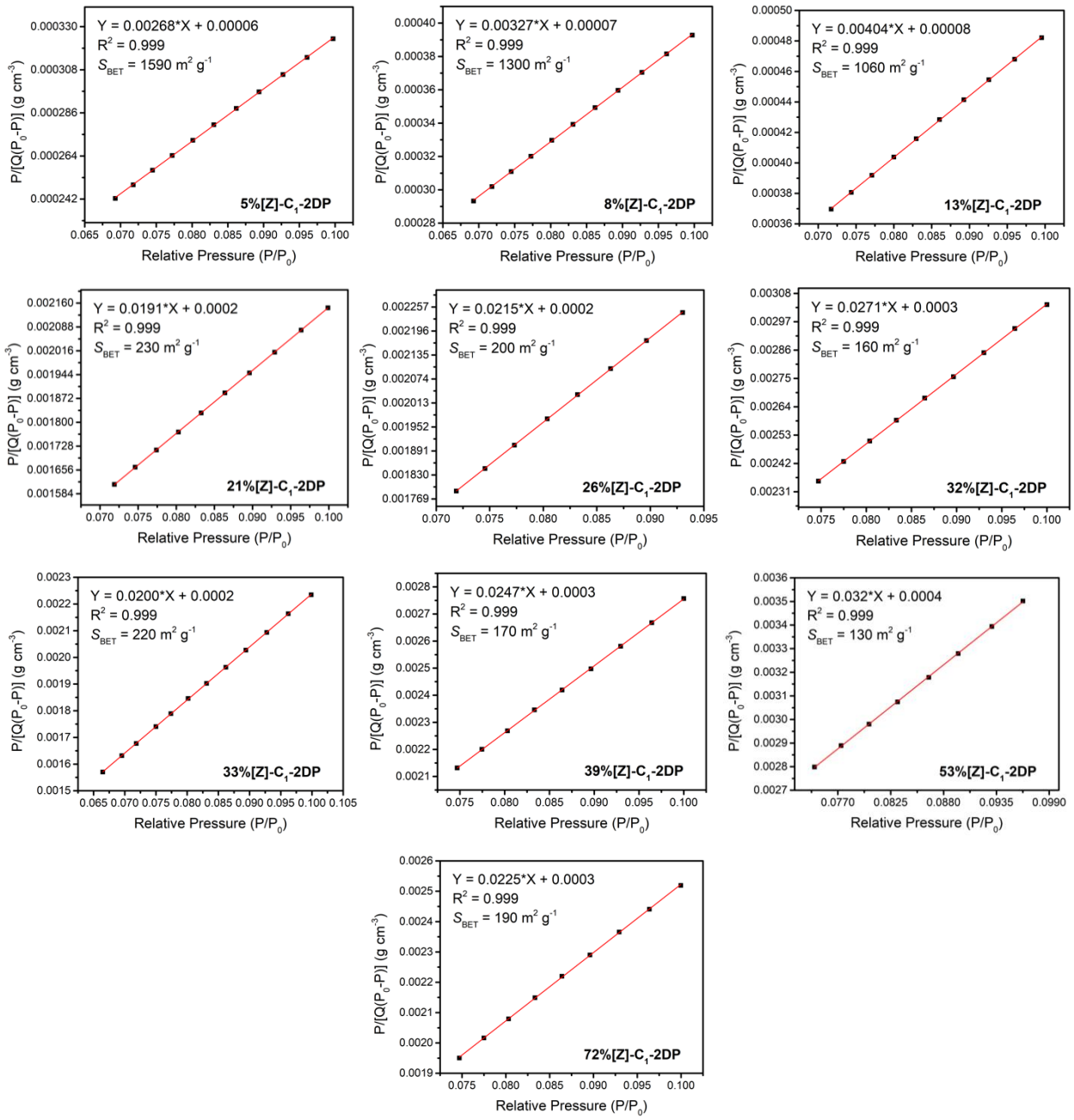

Figure S33. BET plots for **Y_2%[Z]-C_1-2DP**s.

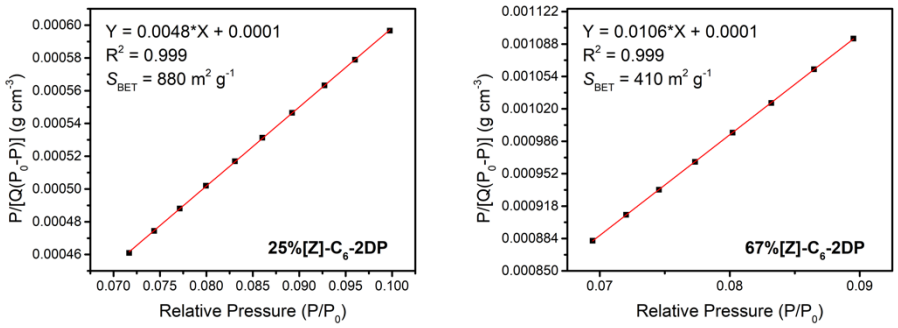

Figure S34. BET plots for **25%[Z]-C6-2DP** and **67%[Z]-C6-2DP**.

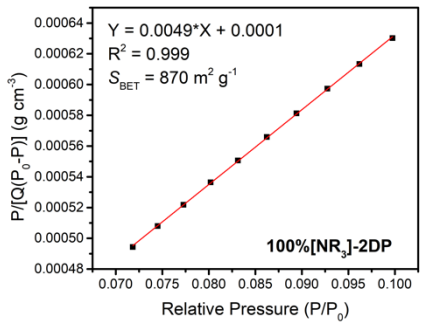

Figure S35. BET plot for **100%[NR3]-2DP**.

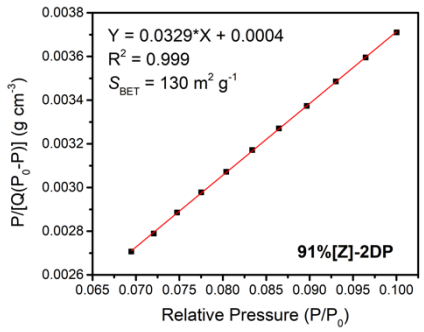

Figure S36. BET plot for **91%[Z]-2DP**.

Nitrogen Porosimetry Data

Table S2. S_{BET} vs. zwitterion loading data of **Y_2%[Z]-C_1-2DP**s from **Figure 3**.

Zwitterion Loading %	S_{BET} (m^2 g^{-1})
5	1590
8	1300
13	1060
21	230
26	200
32	160
33	220
39	170
53	130
72	190

Pore Width Distributions

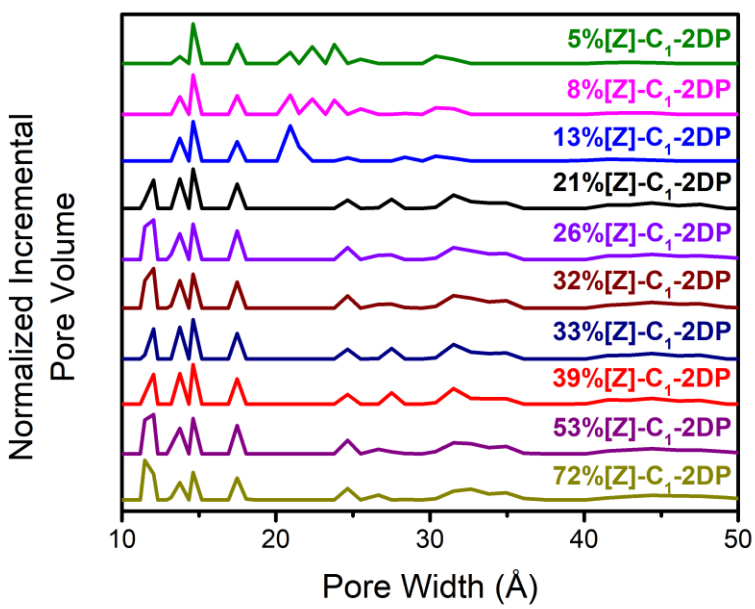

Figure S37. Pore width distributions for **Y_2%[Z]-C_1-2DP**s, using a nonlinear density functional theory (NL-DFT) model.

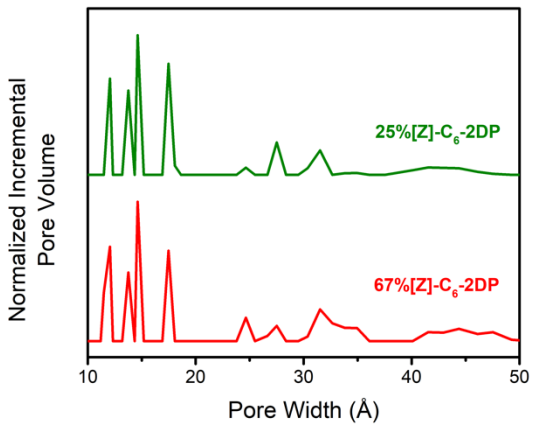

Figure S38. Pore width distributions for **25%[Z]-C6-2DP** and **67%[Z]-C6-2DP**, using NL-DFT.

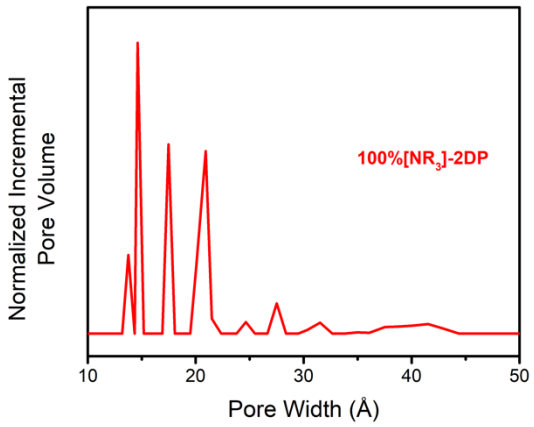

Figure S39. Pore width distribution for **100%[NR3]-2DP**, using NL-DFT.

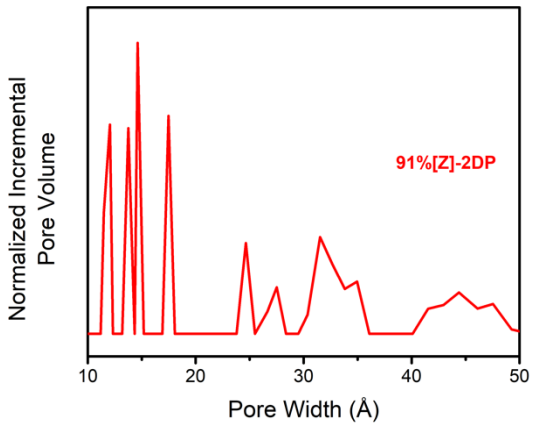

Figure S40. Pore width distribution for **91%[Z]-2DP**, using NL-DFT.

E. FT-IR Data

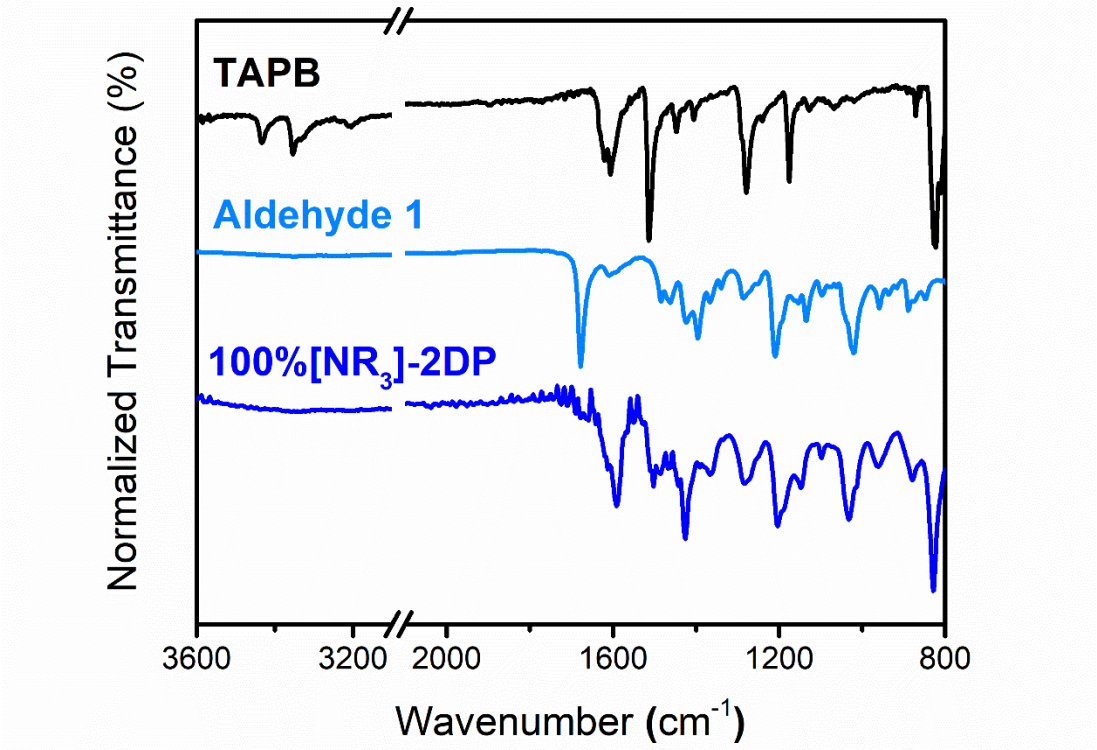

Figure S41. FT-IR data comparing monomers and **100%[NR3]-2DP**. Observed is the disappearance of amine (3350 cm^{-1}) and aldehyde (1680 cm^{-1}) features and the appearance of an imine stretch (1590 cm^{-1}), indicating a high degree of polymerization.

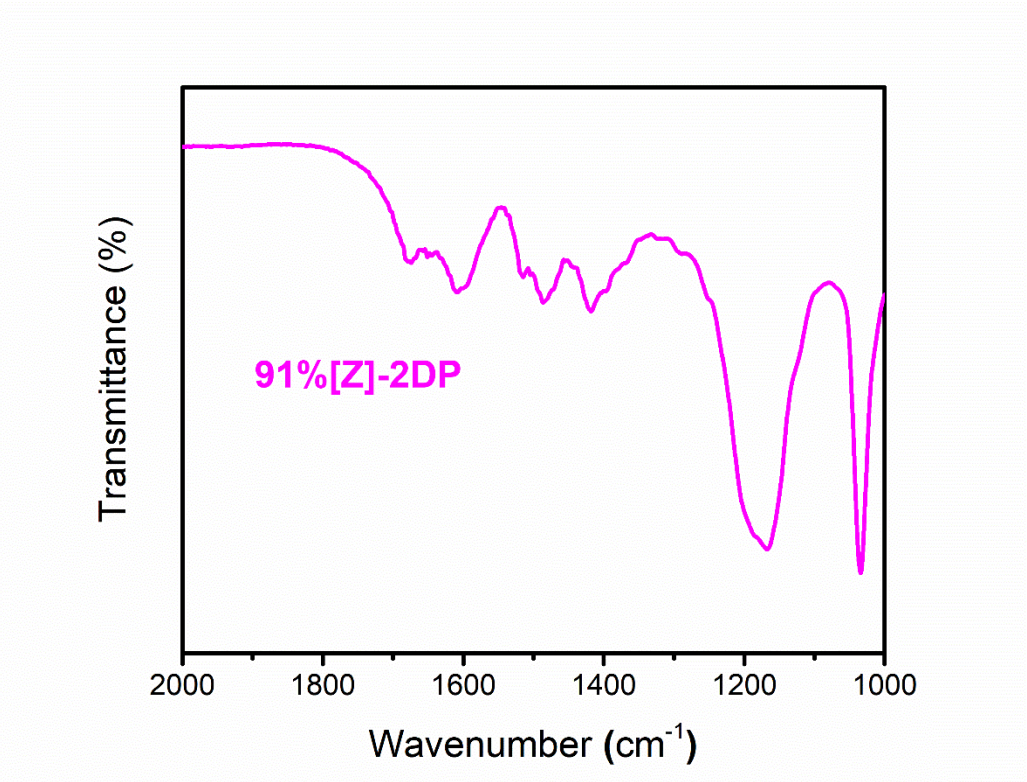

Figure S42. FT-IR data of **91%[Z]-2DP** zoomed into the region containing the imine stretch (1590 cm^{-1}), which is maintained after the zwitterion-forming reaction.

1,3-propane sultone reacts preferentially with the dimethylamine groups, not the imine groups. This is first evident by the high average dimethylamine conversion rates consistently observed. Additionally, the FT-IR and ^{13}C CP-MAS NMR data upon reaction indicates the imine linkages within the 2DP sheets were preserved. Together, these demonstrate the integrity of the imine linkages after the transformation. While it is not possible to completely exclude the possibility that some imine groups reacted with the sultone reagent, this was at most a minor side reaction.

F. NMR Data

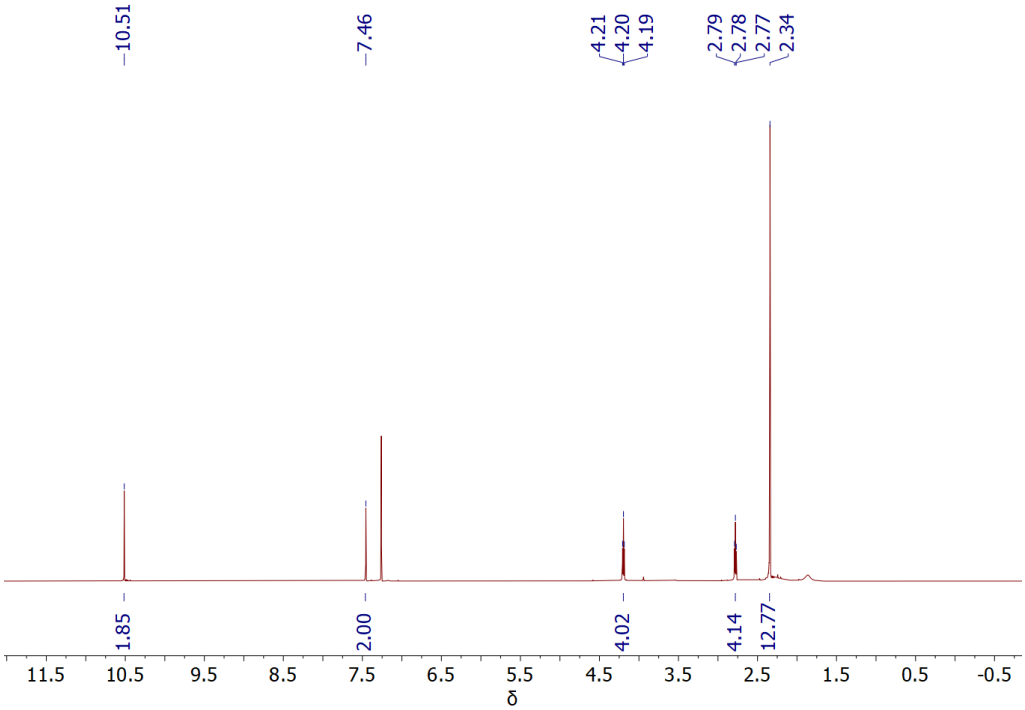

Figure S43. ^{1}H NMR spectrum of **1** in $CDCl_3$.

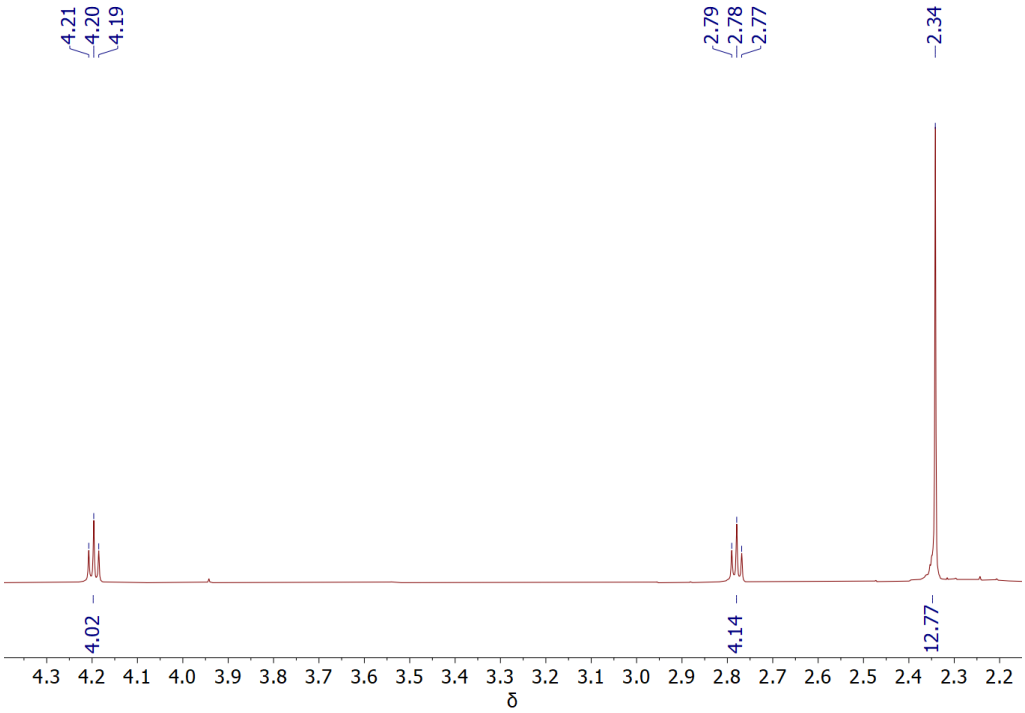

Figure S44. Zoomed-in ^{1}H NMR spectrum of **1** in $CDCl_3$.

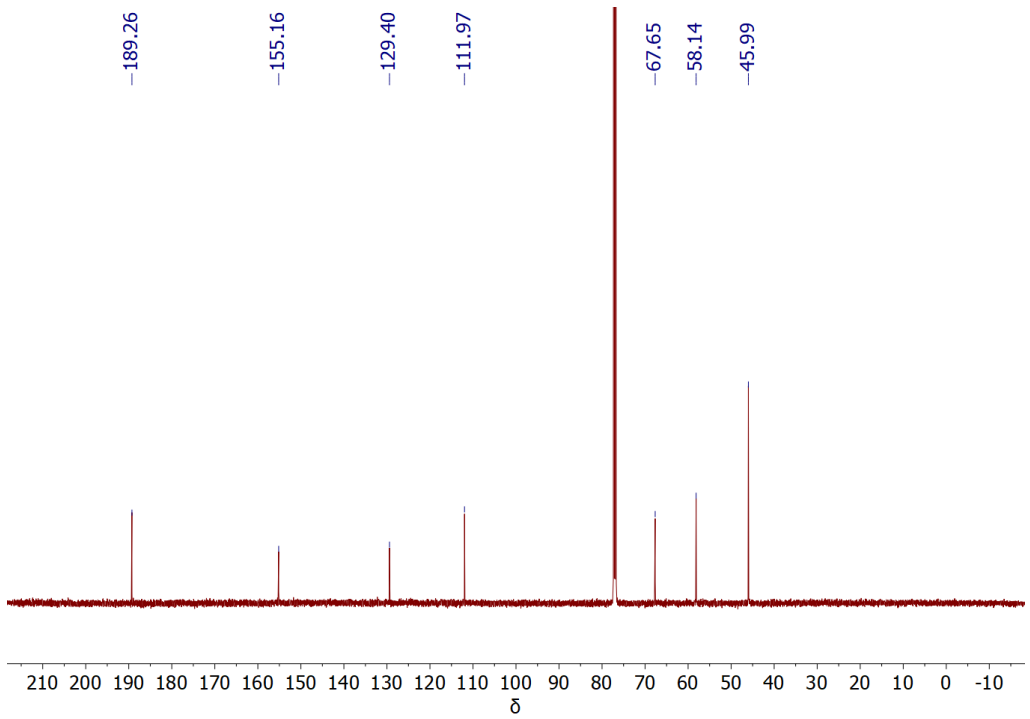

Figure S45. ^{13}C NMR spectrum of **1** in $CDCl_3$.

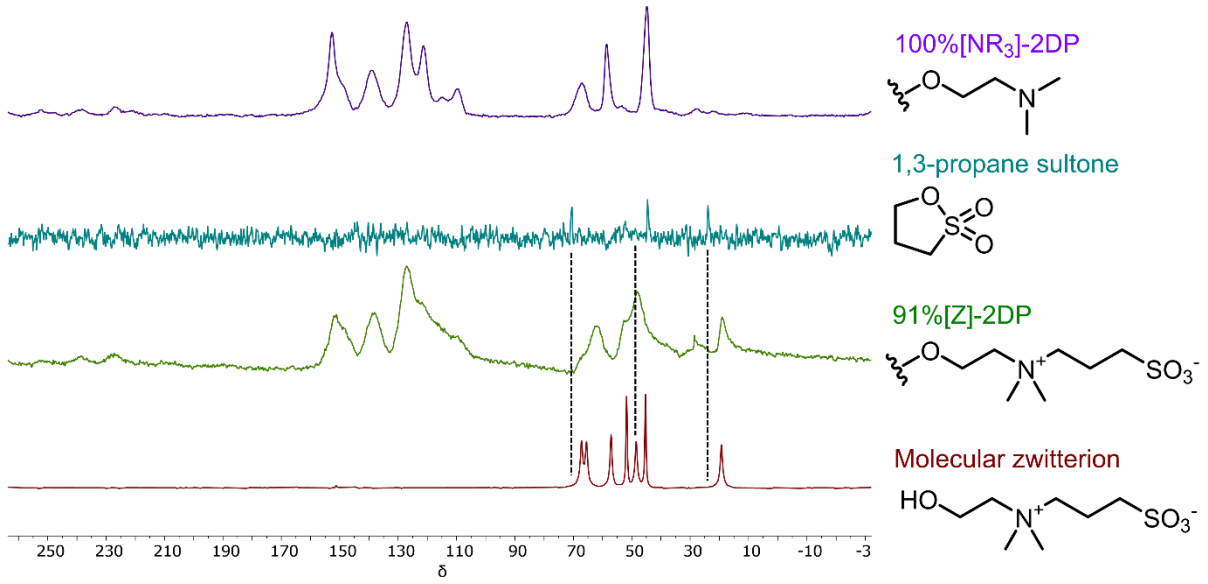

Figure S46. ^{13}C CP-MAS NMR spectra of **100%[NR$_3$]-2DP**, 1,3-propane sultone, **91%[Z]-2DP**, and a commercially available molecular zwitterion. Dotted lines added for clarity. The **91%[Z]-2DP** product peaks upfield of 70 ppm are shifted from the spectra of the starting materials. The spectrum of **91%[Z]-2DP** does not lose any peaks present in the spectrum of **100%[NR$_3$]-2DP**, indicating that the transformation does not damage the 2DP backbone. All spectra were acquired in the solid state.

G. SEM Data

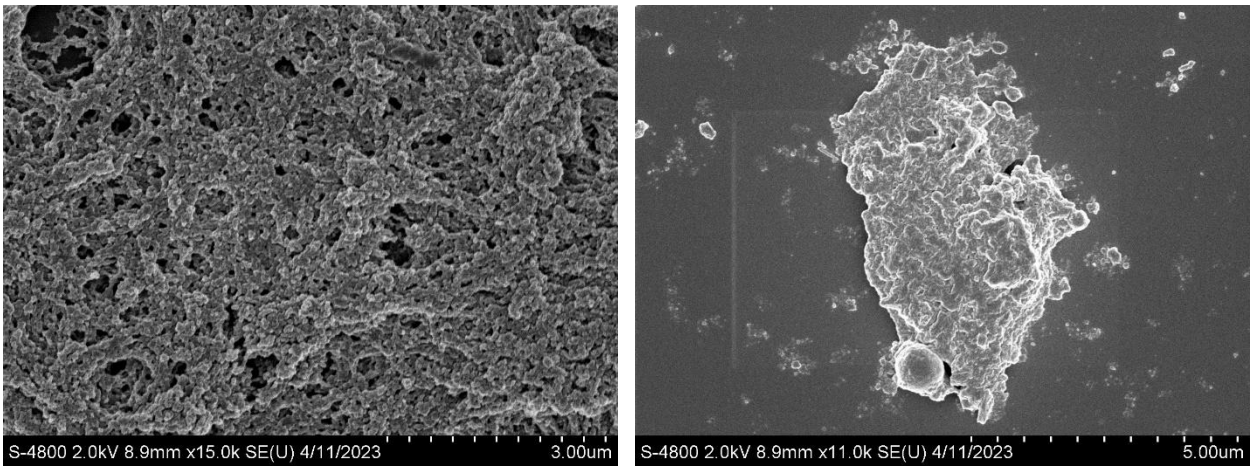

Figure S47. SEM images of **100%[NR_3]-2DP**, which show typical polycrystalline 2DP structure.

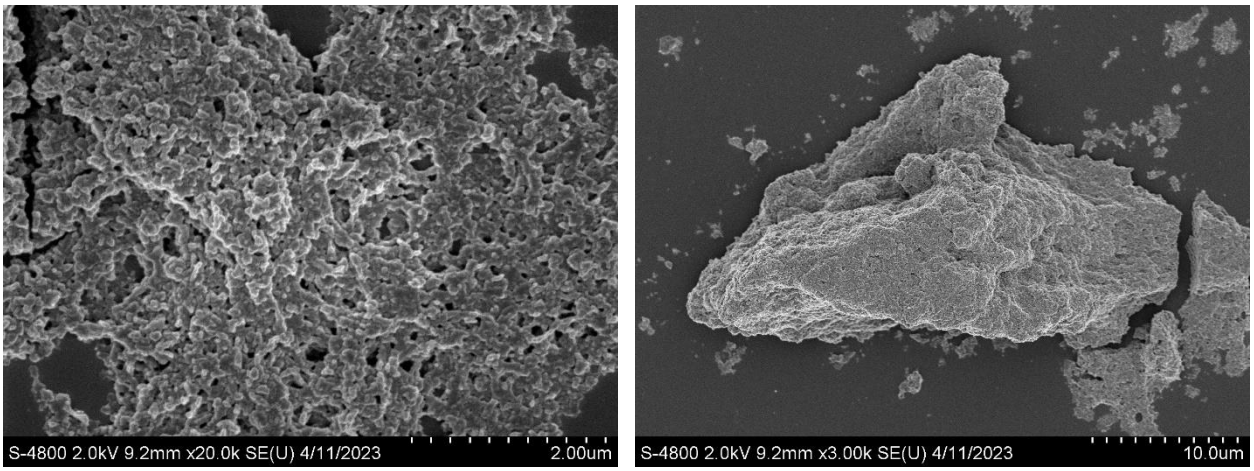

Figure S48. SEM images of **91%[Z]-2DP**, which show typical polycrystalline 2DP structure.

H. References

1. Y. Okada, M. Sugai and K. Chiba, *J. Org. Chem.*, 2016, **81**, 10922-10929.
2. P. Shao, J. Li, F. Chen, L. Ma, Q. Li, M. Zhang, J. Zhou, A. Yin, X. Feng and B. Wang, *Angew. Chem., Int. Ed.*, 2018, **57**, 16501-16505.
3. J. I. Feldblyum, C. H. McCreery, S. C. Andrews, T. Kurosawa, E. J. Santos, V. Duong, L. Fang, A. L. Ayzner and Z. Bao, *Chem. Commun.*, 2015, **51**, 13894-13897.
4. R. L. Li, A. Yang, N. C. Flanders, M. T. Yeung, D. T. Sheppard and W. R. Dichtel, *J. Am. Chem. Soc.*, 2021, **143**, 7081-7087.